AGU PUBLICATIONS

JGR

Journal of Geophysical Research: Solid Earth

RESEARCH ARTICLE

10.1002/2017JB014684

Diffuse Extension of the Southern Mariana Margin

Fernando Martinez[1], Robert J. Stern[2], Katherine A. Kelley[3], Yashuhiko Ohara[4,5], Jonathan D. Sleeper[6], Julia M. Ribeiro[7], and Maryjo Brounce[8]

[1]Hawai'i Institute of Geophysics and Planetology, School of Ocean and Earth Science and Technology, University of Hawai'i at Mānoa, Honolulu, HI, USA, [2]Geosciences Department, University of Texas at Dallas, Richardson, TX, USA, [3]Graduate School of Oceanography, University of Rhode Island, Narragansett, RI, USA, [4]Hydrographic and Oceanographic Department of Japan, Tokyo, Japan, [5]Japan Agency for Marine-Earth Science and Technology, Yokosuka, Japan, [6]Department of Geology and Geophysics, School of Ocean and Earth Science and Technology, University of Hawai'i at Mānoa, Honolulu, HI, USA, [7]Earth Science Department, Rice University, Houston, TX, USA, [8]Earth Sciences Department, University of California, Riverside, CA, USA

Key Points:
- The southern Mariana margin is undergoing diffuse volcano-tectonic extension above a dewatering subducting slab
- This deformation may be analogous to that inferred at subduction zone infancy
- Hydrous convergent margin lithosphere may enable diffuse extension and inhibit narrow plate boundary zone characteristic of plate tectonics

Supporting Information:
- Supporting Information S1

Correspondence to:
F. Martinez,
fernando@hawaii.edu

Citation:
Martinez, F., Stern, R. J., Kelley, K. A., Ohara, Y., Sleeper, J. D., Ribeiro, J. M., & Brounce, M. (2018). Diffuse extension of the southern Mariana margin. *Journal of Geophysical Research: Solid Earth*, *123*. https://doi.org/10.1002/2017JB014684

Received 10 JUL 2017
Accepted 9 JAN 2018
Accepted article online 13 JAN 2018

Abstract Extension within the southern Mariana margin occurs both normal to and parallel to the trench. Trench-normal extension takes place along focused and broad backarc spreading axes forming crust that is passively accreted to the rigid Philippine Sea plate flank to the northwest. To the southeast, trench-parallel extension has split apart the Eocene-Miocene forearc terrain accreting new crust diffusely over a 150–200 km wide zone forming a pervasive volcano-tectonic fabric oriented at high angles to the trench and the backarc spreading center. Earthquake seismicity indicates active extension over this forearc region and basement samples date young although waning volcanic activity. Such diffuse formation of new oceanic crust and lithosphere is unusual; in most oceanic settings extension rapidly focuses to narrow plate boundary zones—a defining feature of plate tectonics. Diffuse crustal accretion has been inferred to occur during subduction zone infancy, however. We hypothesize that in a near-trench extensional setting, the continual addition of water from the subducting slab creates a weak overriding hydrous lithosphere that deforms broadly. This process counteracts mantle dehydration and strengthening proposed to occur at mid-ocean ridges that may help to focus deformation and melt delivery to narrow plate boundary zones. The observations from the southern Mariana margin suggest that where lithosphere is weakened by high water content narrow seafloor spreading centers cannot form. These conditions likely prevail during subduction zone infancy, explaining the diffuse contemporaneous volcanism inferred in this setting.

Plain Language Summary The edges of plates above subduction zones deform diffusely unlike the focused boundaries predicted by plate tectonics to delimit oceanic lithosphere. This diffuse deformation has been mapped in a presently active rift within the overriding plate behind the southern Mariana trench and appears to be due to weakening effects of water released by the subducting plate. The southern Mariana margin may represent an active analog of the broad and diffuse deformation and volcanism inferred to occur at the earliest stages of subduction zone formation. The observations also suggest that mantle dehydration thought to accompany melting at mid-ocean ridges may be an important process in forming the focused plate boundary zones characteristic of plate tectonics. Such dehydration apparently cannot occur along the upper plate edges of subduction zones due to continually dewatering subducting slabs.

1. Introduction

The conjugate rifted margins that border backarc basins are quite unlike the margins of continental rifts. The jigsaw puzzle-like fit of continental margins bordering the Atlantic Ocean (Wegner, 1966) was among the first observations leading to the theory of plate tectonics. In contrast, the rifted margins of backarc basins frequently show large geometric discrepancies belying their conjugate nature. A type example is the Izu-Ogasawara (Bonin)-Mariana-Yap (abbreviated IBM hereafter) forearc, which is the conjugate of the remnant arc Kyushu-Palau Ridge (Karig, 1972; Seno & Maruyama, 1984; Taylor, 1992). A visual inspection of the trace of these features shows that they cannot be joined by a rigid-plate Eulerian rotation of their present outline (Figure 1), even taking into account the complex opening history of the Parece Vela and Shikoku Basins (Okino et al., 1998, 1994). This incongruence developed because the two flanks of the basin behaved differently during opening. The trailing flank became a passive part of the rigid Philippine Sea plate as it was accreted, and it preserved the original geometry of the arc system and of the crust spread from the

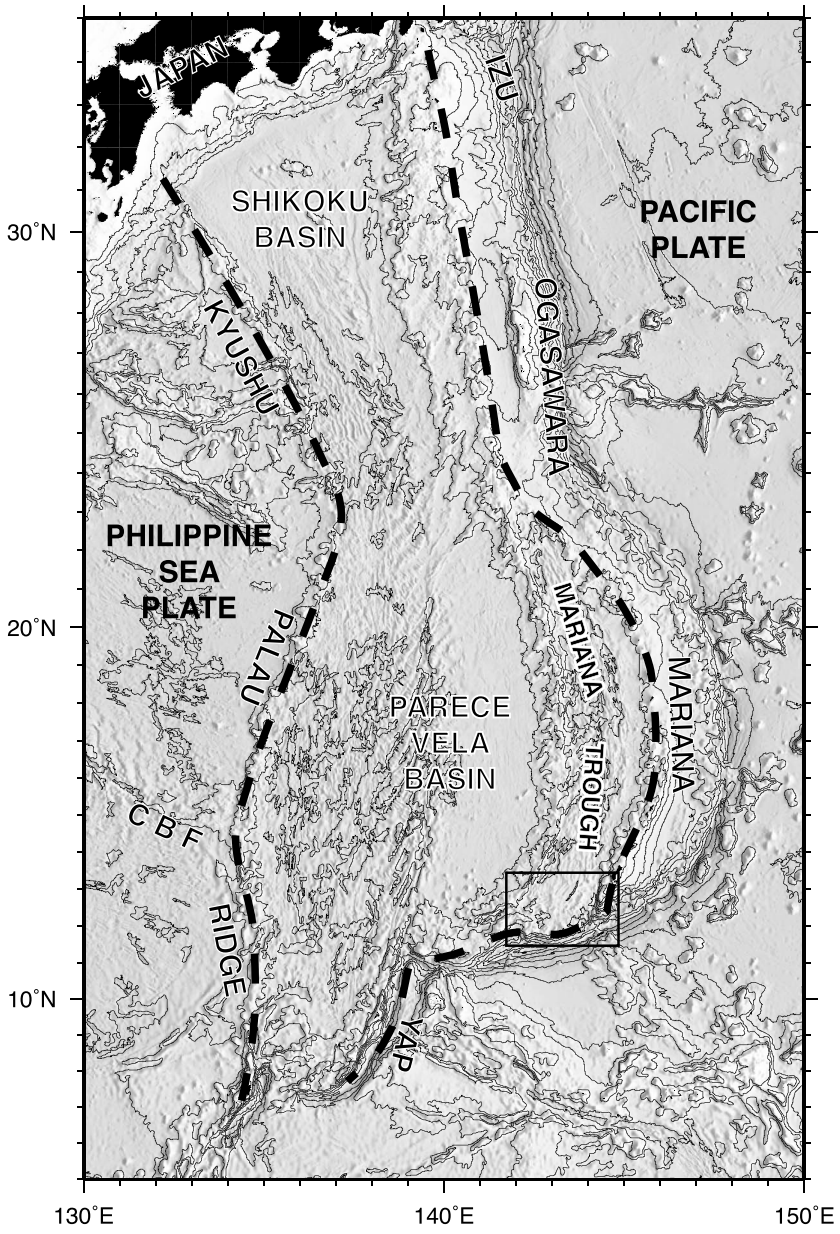

Figure 1. The rifted edges of the Izu-Ogasawara (Bonin)-Mariana-Yap (IBM) forearc and remnant Kyushu-Palau Ridge (KPR), indicated with dashed lines, were joined before the opening of the Shikoku and Parece Vela Basins and Mariana Trough, yet they cannot be reassembled by rigid-plate Eulerian rotation of their present shapes. Whereas the KPR remained fixed to the rigid Philippine Sea plate, retaining the original shape of the margin, the conjugate eastern margin was deformed as the trench changed shape during opening of the various backarc basins. The large change in shape between conjugate margins indicates a weak leading edge of the subduction margin lithosphere that conforms to a changing trench geometry. CBF locates the Central Basin Fault, which was an active spreading center during subduction initiation and infancy, but had ceased activity by the time of KPR rifting. The box at the southern end of the Mariana Trough outlines the study area.

backarc spreading centers. In contrast, the leading flank (between the backarc spreading center and the trench) deformed as the backarc basin opened.

The changing shape of the leading edge of subduction margins has several causes. One is that the subducting plate must undergo large strains in order to subduct (Bevis, 1988) and in general cannot be torsionally rigid (Bevis, 1986). This means that the plate boundary zones bordering subduction margins undergo large lithospheric deformations and that the map view shape of the trench is not constrained by rigid plate kinematics, but can change as backarc basin opening progresses. A second inference is that the leading edge of

the upper plate is weak and deforms to conform to the changing shape of the trench. Although weakening of forearc mantle material accompanies serpentinization (Hyndman & Peacock, 2003), this is not the only cause. Weakening of the upper plate margin may also be due to effects of water on crystal lattice deformation mechanisms in olivine (Karato et al., 1986; Mei & Kohlstedt, 2000a, 2000b) that have been proposed to lower the strength of not only the upper plate lithosphere (Hirth & Kohlstedt, 1996) but also of the mantle wedge asthenosphere (Billen & Gurnis, 2001; Hirth & Kohlstedt, 2003).

Here we examine the southern Mariana margin—the area south of about the latitude of Guam (13°30′N) and extending from the West Mariana Ridge to the trench. This area is floored by young (<5 Myr) accreted volcanic material erupted following rifting of the Eocene-Miocene forearc away from the West Mariana Ridge and parallel to the trench. Thus, in the southern Mariana margin, the region of "backarc" crustal accretion traditionally called the Mariana Trough is expanded to include areas of new volcanic crustal accretion approaching the trench, where fragments of the Eocene-Miocene forearc may remain. We also use the term "Mariana platelet" to refer to the lithosphere between the Philippine Sea plate and the Pacific plate. "Platelet" here, however, is intended to not only denote a narrow lithospheric sliver but one that is also deforming and is not therefore truly a "plate." Martinez et al. (2000) referred to this region as the "interplate" zone and Bird (2003) as the "Mariana Plate" but Mariana platelet has been traditionally used to refer to this area (e.g., Eguchi, 1984; Karig et al., 1978) and is used herein.

Although models of backarc opening generally treat trenches and slabs as retreating oceanward in a mantle framework (Molnar & Atwater, 1978), regional plate motion models indicate that the IBM trenches and slabs are actually advancing continentward toward Eurasia (Carlson & Melia, 1984; Carlson & Mortera-Gutiérrez, 1990). Modern geodetic measurements, in fact, show that all the tectonic components of the IBM area—the forearc platelet, Philippine Sea plate, and Pacific plate—are advancing westward toward Eurasia (Kato et al., 2003; Kobayashi, 2004) whether or not the adjacent margin is undergoing backarc opening. Extension in the Mariana Trough results from a lag in motion of the trench with respect to the Philippine Sea plate (Carlson & Melia, 1984; Kato et al., 2003) and possible outflow of asthenospheric mantle from beneath a shrinking Philippine Sea plate (Ribeiro et al., 2017). Following Carlson and Melia (1984) we refer to the lagging trench motion relative to the Philippine Sea plate as trench rollback. However, this rollback is caused not simply by the Philippine Sea plate moving away from a fixed-shape trench. The overall Mariana frontal arc has significantly changed shape and curvature as it roughly moves eastward relative to the remnant West Mariana Ridge (Karig et al., 1978) in the ~5 Myr since Mariana Trough spreading began (Hussong & Uyeda, 1981). In the southern Mariana margin, trench rollback has both eastward and southward directed components. Purely kinematic arguments predict that rollback is directed normal to the trend of the trench and is not affected by the relative motion between subducting and overriding plates (Dewey, 1980). However, other factors may influence changes in the shape of the trench. Geologic features such as plateaus, seamounts, seamount chains, and other features on the subducting plate can change the shape of the trench as they impinge on it and variably resist subduction (e.g., Wallace et al., 2009). In addition, mantle transition zone discontinuities at depth can resist slab penetration and affect the motion and shape of the trench (Schellart, 2004). Poorly understood local dynamic flow effects between mantle and slab as well as possible regional mantle flow relative to the slab may also affect changes in trench motion and shape (Ribeiro et al., 2017; Schellart & Moresi, 2013). Nevertheless, as we show in section 3.2 from earthquake focal mechanisms, the current rollback motion of the Mariana subduction interface is to first order nearly perpendicular to the local trend of the trench as predicted by kinematic theory (Dewey, 1980). In contrast, the trench-parallel component of motion along the subduction interface, which appears to be the greater component based on geodetic measurements and plate motion models (Kato et al., 2003), has a much smaller teleseismic expression.

We discuss below two main domains of extension and crustal accretion within the southern Mariana margin. In one domain, trench-normal extension and crustal accretion are taken up as seafloor spreading on the narrow axis of a backarc ridge, the Malaguano-Gadao Ridge (MGR), and continues westward as a broader diffuse spreading zone (DSZ) tens of kilometers wide (Figure 2). This domain forms the NW flank material accreted to the rigid Philippine Sea plate (Figure 2). The other domain is located between the MGR/DSZ and the trench. In this domain, trench-parallel (tangential) extension is broadly distributed in a zone over ~200 km wide forming a pervasive volcano-tectonic fabric oriented at a high angle to both the trench and backarc spreading center. While some of this material may have spread from the MGR/DSZ, the predominance of high-angle basement fabric indicates that significant volcanic crust was accreted due to trench-parallel extension of the margin.

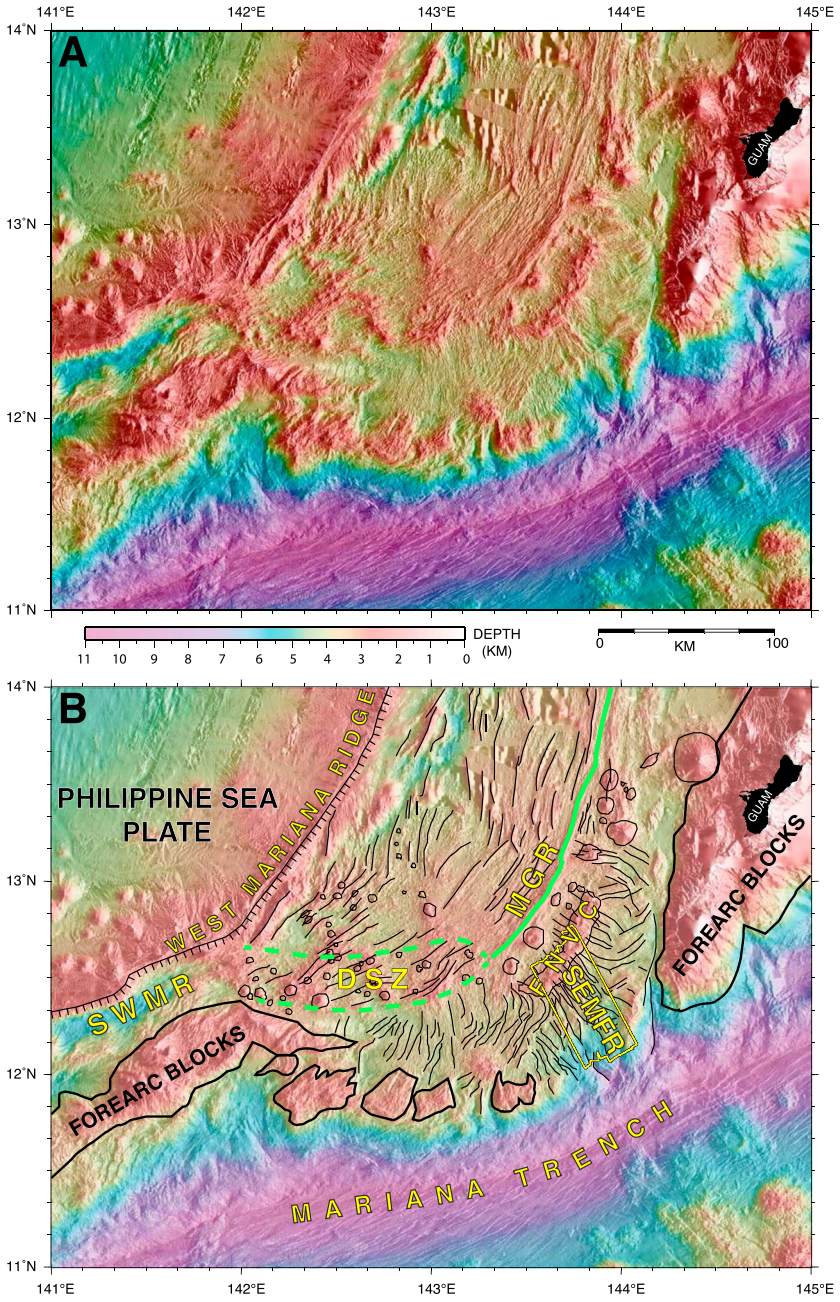

Figure 2. Shaded relief image of the southern Mariana margin illuminated from the east. (a) The bathymetry map is compiled from multibeam data from the University of New Hampshire Law of the Sea Project (Armstrong, 2011) supplemented with data from the U.S. National Geophysical Data Center, Japan Agency for Marine Earth Science and Technology, and R/V *Thomas G. Thompson cruise TN273* data. (b) Interpreted features. The yellow outline shows area of IMI-30 deep-towed side scan sonar imagery (Figure S1). The green line is the Malaguana-Gadao Ridge (MGR), and the dashed outlined region is the diffuse spreading zone (DSZ). SWMR is the Southwest Mariana Rift. The fine lines indicate basement fabric trends. The bold lines outline interpreted fragments of the Eocene-Miocene forearc. The southern margin between the MGR/DSZ and the trench is the diffuse zone of margin extension characterized by pervasive volcano-tectonic fabric at a high angle to the trench and spreading center.

Ongoing broad deformation of the southern Mariana margin may be an active analog of the contemporaneous and widely distributed (~300 km wide) magmatic crustal accretion proposed to have occurred during the subduction zone infancy of the IBM system (Arculus et al., 2015; Ishizuka et al., 2006; Stern & Bloomer, 1992; Taylor, 1992). In both settings, mantle hydration from the underlying dewatering slab should weaken

the lithosphere (Hirth & Kohlstedt, 1996) and lower the peridotite solidus (Gaetani & Grove, 1998; Grove et al., 2012). Farther from the trench, however, water release from the slab decreases (Schmidt & Poli, 1998), thus decreasing hydration of the mantle wedge as indicated by water content in erupted backarc basin lavas (Kelley et al., 2006). Extension is eventually localizes at a narrow plate boundary zone formed in less hydrous and therefore stronger mantle lithosphere. Our findings imply that hydrous oceanic lithosphere deforms broadly, in support of inferences that the narrow plate boundary zones of oceanic seafloor spreading centers are at least partly enabled by melting and melt extraction leading to dehydration strengthening of the residual mantle (Hirth & Kohlstedt, 1996; Phipps Morgan, 1997).

2. Methods and Data

We conducted a marine geophysical and rock sampling expedition on R/V *Thomas G. Thompson* from 22 December 2011 to 22 January 2012 in the southern Mariana margin (Cruise TN273). The survey focused on the deeper rifted area within the southeast part of the margin, referred to as the Southeast Mariana Forearc Rifts (SEMFR) (Ribeiro, Stern, Kelley, et al., 2013). The geophysical components included seafloor mapping with a hull-mounted Kongsberg EM302 multibeam system, magnetic data acquisition with a towed magnetometer, and deep-towed side scan sonar mapping with the 30 kHz IMI-30 vehicle (Rognstad et al., 2003). The IMI-30 was deployed in two main survey areas—along the Malaguana Gadao Ridge (MGR), the magmatically inflated southern Mariana backarc seafloor spreading center (Becker et al., 2010), and the SEMFR area (Figure 2) at the eastern end of the rifted margin. A 1 day survey of the Shinkai Seep (Ohara et al., 2012), a serpentinite-hosted fluid seep in the outer trenchward slope, was also performed (Stern et al., 2014). Geophysical results from the MGR and its westward continuation as the diffuse spreading zone (DSZ) extending to the Southwest Mariana Rift (SWMR, Figure 2) are reported in a manuscript in preparation: "Diffuse spreading, a new mode of crustal accretion in the southern Mariana Trough backarc basin" by J. D. Sleeper, F. Martinez, R. J. Stern, P. Fryer, K. Kelley, and Y. Ohara. Results of the geochemical sampling in the SEMFR area and surrounding margin are reported in Ribeiro, Stern, Martinez, et al. (2013), Ribeiro, Stern, Kelley, et al. (2013), Ribeiro et al. (2015, 2017), and Brounce et al. (2014). A geochemical study of the rifted arc volcanic front in this area, the Fina Nagu Volcanic Chain (FNVC; Figure 2), is given in Brounce et al. (2016). Here we discuss the geophysical component of the cruise focusing on the margin seaward of the backarc spreading center area in the context of the broader southern Mariana margin.

2.1. Multibeam Data

To examine the regional setting beyond the detailed area of the near-bottom side scan sonar survey, we compiled available archive multibeam data. These include systematic bathymetric mapping of the southern margin extending from east of the trench to west of the West Mariana Ridge acquired by a U.S. Navy hydrographic vessel (Armstrong, 2011) and archived at the University of New Hampshire, Center for Coastal and Ocean Mapping (http://ccom.unh.edu/theme/law-sea). Additional multibeam bathymetry data were added from our R/V *Thompson* cruise (TN273), as well as the U.S. National Geophysical Data Center (now National Centers for Environmental Information), and Japan Agency for Marine-Earth Science and Technology (JAMSTEC) data archives where they expanded the coverage or improved the resolution. The combined regional data sets (Figure 2) were gridded at 0.001° in latitude and longitude (~100 m) and at 0.0003° (~30 m) in the area of the 30 kHz EM302 data (Figure S2 in the supporting information).

2.2. Earthquake Teleseismic, Geodetic, and Plate Motion Data

To investigate the southern Mariana margin tectonics, we compiled earthquake focal mechanism and hypocenter data from the Global Centroid Moment Tensor (CMT) project (Dziewonski et al., 1981; Ekström et al., 2012) and the International Seismological Centre (ISC) online bulletin (International Seismological Centre, 2014) respectively. To isolate earthquake focal mechanisms associated with the subduction interface and upper plate and exclude deep slab events, we limit CMT hypocenter depths to 80 km or less. We plot thrust focal mechanism solutions along with their compressional *p*-axis azimuths in red and normal and strike-slip events and their tension *t*-axis azimuths in blue for the entire Mariana margin (Figure 3) and in detail for the southern margin (Figure 4). Earthquake epicenter locations from the ISC bulletin for magnitudes greater than 5 and depths of 80 km or less are also shown in Figures 3 and 4. We also plot Global Positioning System (GPS) geodetic vectors relative to Eurasia and the Philippine Sea plate from Kato et al. (2003) in Figure 3 along with contours of Pacific plate motion relative to the Philippine Sea plate. An expanded view and interpretation of

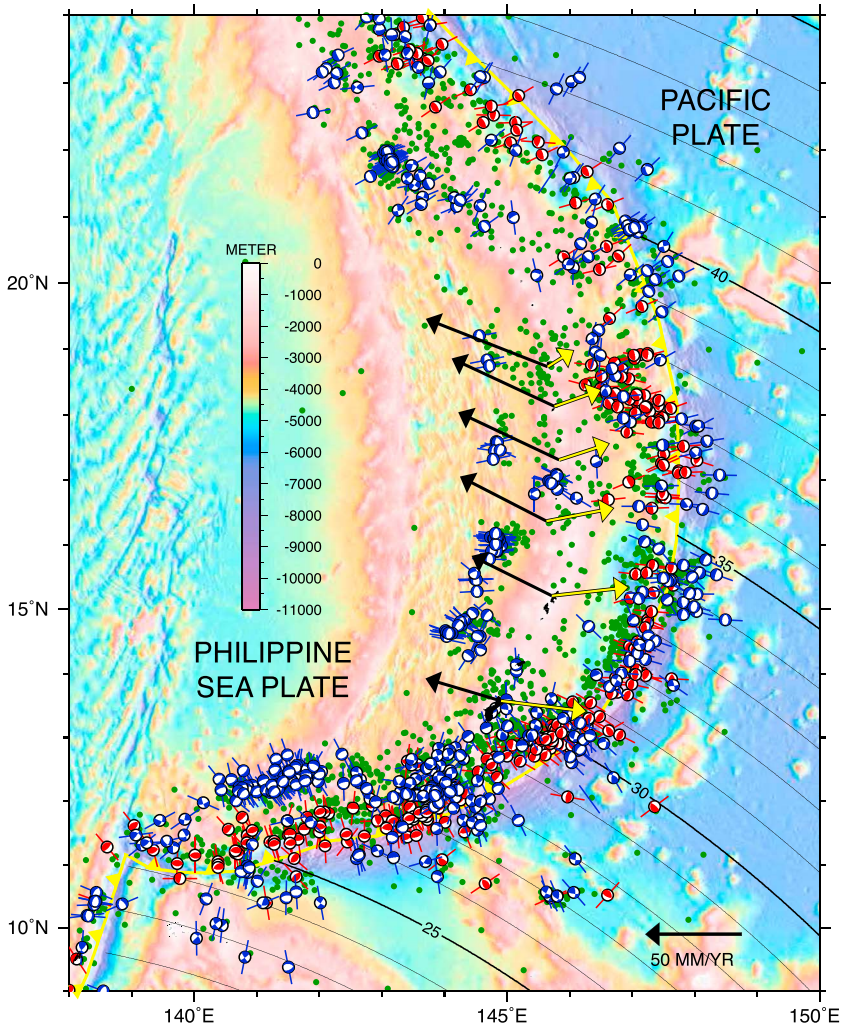

Figure 3. Kinematics and seismotectonics of the Mariana margin. Earthquake focal mechanisms from the Global CMT project with depths of 80 km or less are shown. Thrust mechanisms and their *p*-axis azimuths (bars) are colored red; normal and strike-slip mechanisms and their *t*-axis azimuths (bars) are colored blue. Also shown are epicenters from the International Seismological Center (green dots) for depths less than 80 km and magnitudes ≥5. The contours are small circles of the Pacific plate motion with respect to the Philippine Sea plate annotated in mm/yr following the Euler pole of Kato et al. (2003). The black and yellow arrows are geodetic vectors determined by Kato et al. (2003) for Mariana island stations with respect to Eurasia and the Philippine Sea plate, respectively (scale at lower right). The approximately normal orientation of the thrust earthquake *p*-axis to the trench indicates that rollback is normal to the trench (yellow line) despite the curving geometry of the trench and changing obliquity of convergence of the Pacific plate.

the teleseismic earthquake and geodetic data for the southern Mariana margin study area are given in Figure 4.

2.3. Gravity Data

To examine large-scale crustal thickness variations in the southern Mariana margin, we derived the mantle Bouguer anomaly (MBA) using the nearly full-coverage multibeam data (Figure 2) and a 1 min satellite-derived free air gravity anomaly grid (version 24.1) (Sandwell et al., 2014). A density contrast of 1,700 kg/m^3 was used for the water/seafloor interface and 600 kg/m^3 for the Moho interface assuming a uniform 6 km thick crust. The geographic (longitude, latitude) bathymetry grids were converted to meters (x, y) using a transverse Mercator projection with a central meridian in the middle of the grid. The gravity effects of the density interfaces (water/seafloor and crust/Moho) were forward calculated using five terms in a three-dimensional fast Fourier transform implementation (Shin et al., 2006) of the Parker (1972) method. The

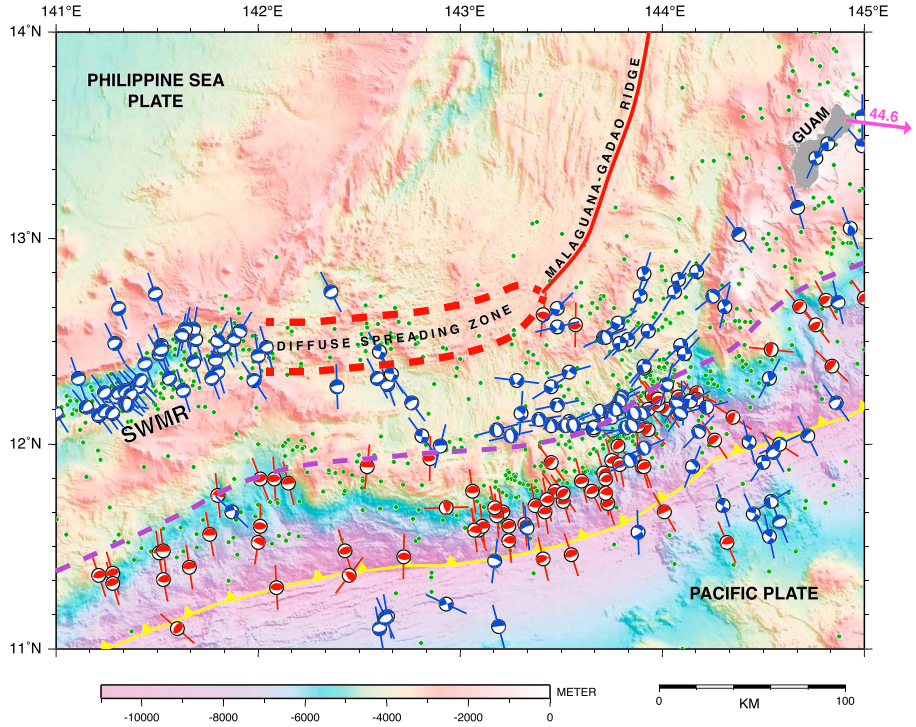

Figure 4. Seismotectonics of the southern Mariana margin. Earthquake data are for depths ≤80 km and magnitudes ≥5. Centroid Moment Tensor solutions from the Global CMT project showing best fit double-couple mechanisms and *p*-axis azimuths for thrust events in red and focal mechanisms and *t*-axis azimuths for normal and strike-slip events in blue. The green dots are International Seismological Center epicenters. The zone of distributed earthquakes delineates the ~200 km wide diffuse deformation zone within the margin south of the organized and diffuse spreading center. The purple arrow at Guam shows the GPS vector relative to the Philippine Sea plate in mm/yr from Kato et al. (2003). Note that thrust *p*-axis azimuths near the trench are generally oriented orthogonal to the trench, whereas the *t*-axis azimuths within the deforming margin are largely oriented subparallel to the trench and backarc spreading center. The region between the trench (yellow line with front symbols) and the purple dashed line delineates the inferred seismogenic subduction interface characterized by thrust events.

gravity effects of the water/seafloor interface and crust/mantle interface were removed from the free air anomaly grid to yield the MBA (Figure 5). The MBA map (Figure 5) retains the effect of the slab, which we have not attempted to remove. Previous studies (Watts & Talwani, 1975) show that slab gravity effects are generally poorly constrained but are expected to have small amplitude and long wavelength because of the small slab/mantle wedge density contrast and great slab depth compared to the crustal sources that we are mostly interested in here. We have also not attempted to remove thermal effects and estimate residual gravity anomalies to derive crustal thickness variations from these anomalies, as is typically done in mid-ocean ridge studies (e.g., Kuo & Forsyth, 1988). Thermal structure and crustal and lithospheric density variations are poorly constrained in this setting with contrasting crustal lithologies, lithospheric ages, and unknown slab effects. Instead, we view the MBA anomaly as a qualitative map depicting major crustal thickness variations. However, we broadly estimate possible crustal thickness variations by comparison with other areas of the Mariana margin where seismic or other determinations have been made.

2.4. Magnetic Data

We examined the available magnetic data to gain an understanding of volcanic crustal accretion processes. At mid-ocean ridges where crust accretes in narrow plate boundary zones and spreads outward from these axes, magnetic anomalies are lineated, show narrow polarity transition widths, and can be correlated with geomagnetic reversal sequences (Harrison, 1987). Thus, the character of the magnetic anomalies reflects the nature of the crustal accretion process.

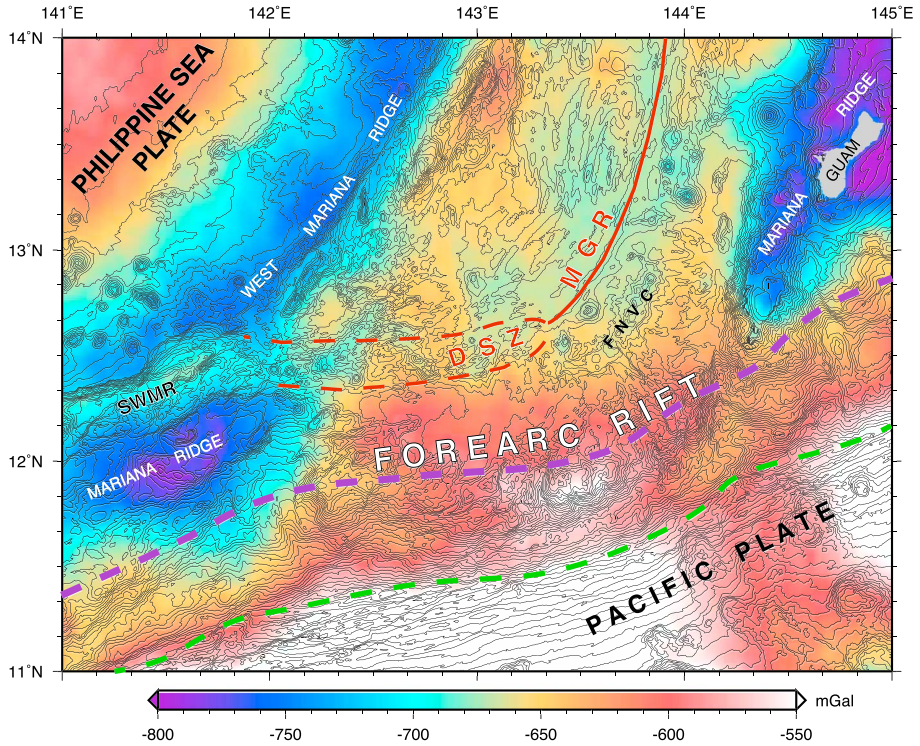

Figure 5. Mantle Bouguer anomaly (MBA) of the southern Mariana margin with 250 m bathymetry contours superimposed for reference. The green dashed line marks the trench axis. The purple line marks the estimated limit of the subduction interface based on thrust earthquakes (see Figure 4). The red solid and dashed line marks the organized and diffuse spreading axes, respectively, which end in tectonic rifting in the southwest Mariana rift (SWMR). MBA lows (blue color) are associated with thick crust of the Mariana Ridge forearc near Guam, and the West Mariana Ridge remnant arc. In contrast, the area labeled "forearc rift" shows MBA highs (red to white) indicating thinner crust. Pacific plate seaward of the trench shows high values due to unaccounted lithospheric thermal structure from the much older plate there.

Due to low ship speed (1–2 knots) during IMI-30 surveys, we could not simultaneously deploy the ship-towed magnetometer. However, upon IMI30 recovery, we conducted a towed magnetometer survey of the SEMFR area at 10 knots, paralleling the IMI-30 tracks. Total force magnetic data were reduced to anomaly by removing the International Geomagnetic Reference Field (Maus & Macmillan, 2005) using GMT software (Wessel et al., 2013). The Thompson data were used as a reference to adjust archive data from the U.S. National Geophysical Data Center and Japan Agency for Marine-Earth Science and Technology (JAMSTEC), which crossed the Thomson magnetic tracks. In most cases a single constant offset was used to remove the average discrepancy with the Thompson data, but for two cruises (R/V *Moana Wave cruise MW9603* and R/V *Yokosuka Cruise YK10-12*) the ship data were broken into straight line segments and offsets were applied on a line-by-line basis. Due to the low inclination (dip) of the ambient and axial geocentric dipole field in this area, small discrepancies between surveys become amplified in the magnetic reductions. To further minimize artifacts created by short wavelength discrepancies, we excluded the regional data from within 3.7 km of the dense R/V *Thompson* data as it already has high density and addition of regional data added artifacts without increasing resolution. Remaining gaps in ship magnetic coverage were filled with a 3 min global grid of ship anomaly data (Lesur et al., 2016).

The bathymetry in the area is shown in Figure 6a for reference, and the compiled magnetic anomaly grid (0.25 min spacing in latitude and longitude) is shown as a color contoured map in Figure 6b. In the study area, the Earth's predicted main field and magnetization vector from the International Geomagnetic Reference Field and axial geocentric dipole hypothesis have low inclinations (approximately 10° and 24°, respectively). This skews the observed anomalies, displacing magnetic lows and highs from their source bodies. To minimize this effect, we carried out a reduction to the pole (Blakely, 1995) of the anomaly field (Figure 6c) followed by an inversion for seafloor magnetization (Parker & Huestis, 1974) (Figure 6d) in Mirone software

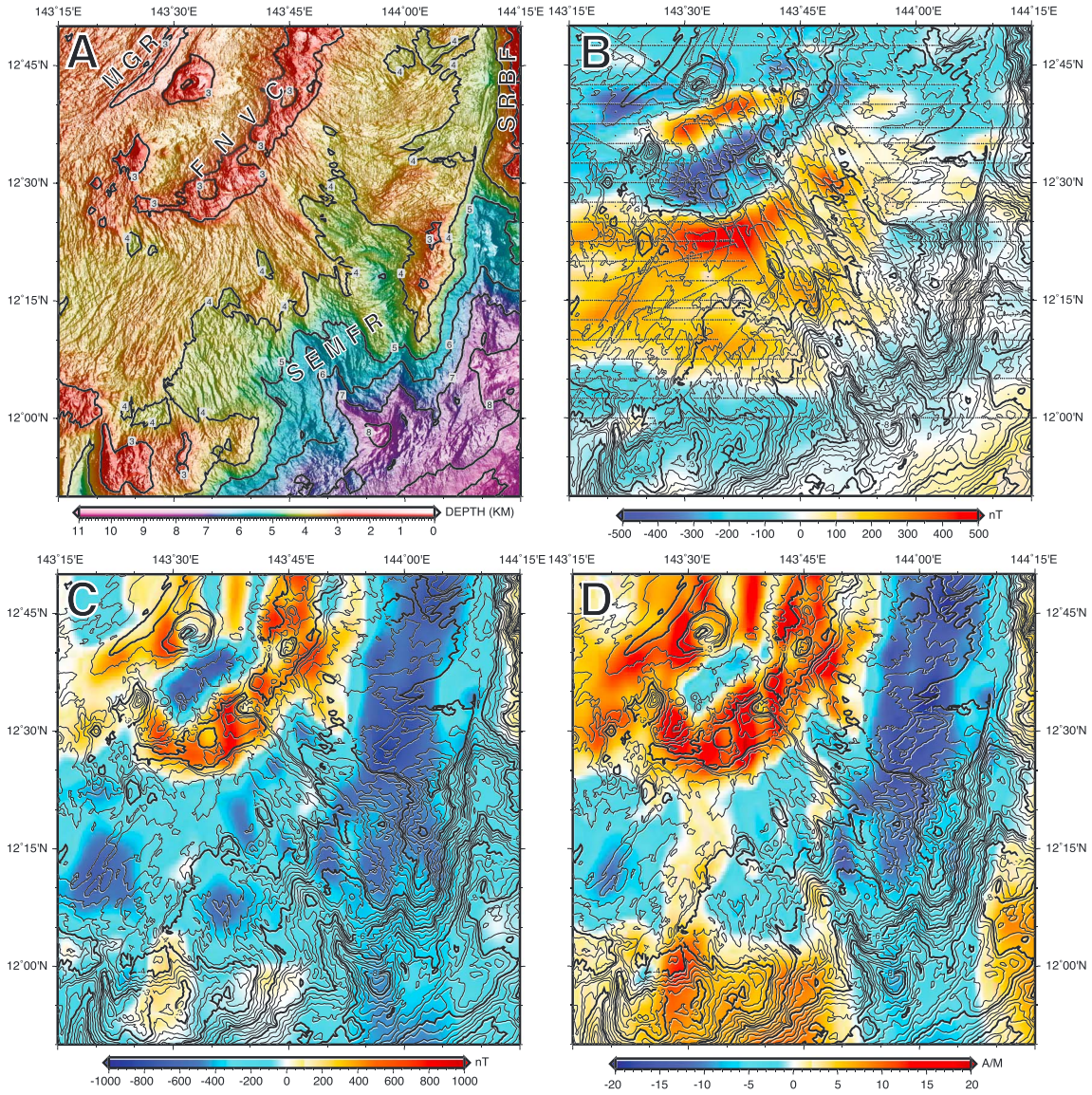

Figure 6. Magnetic reductions. (a) Multibeam bathymetry illuminated from east with 1 km contours. MGR = Malaguano-Gadao Ridge; FNVC = Fina Nagu Volcanic Chain; SEMFR = Southeast Mariana Forearc Rift; SRBF = Santa Rosa Bank Fault (b) Total-field magnetic anomaly showing ship track data used. A 3 min gridded database of magnetic anomaly data (World Digital Magnetic Anomaly Map, http://www.wdmam.org) was used to fill gaps. Data were median filtered and gridded at 0.25 min spacing using a minimum curvature routine (Smith & Wessel, 1990). (c) Magnetic anomaly field reduced to the pole and (d) inverted for seafloor magnetization using the multibeam bathymetry grid employing Mirone software (Luis, 2007). The 200 m bathymetry contours are shown in Figures 6b–6d for reference. Note the pronounced skewness in the anomaly field (Figure 6b), which is removed by reduction to the pole (Figure 6c) and inversion for magnetization (Figure 6d) so that spreading center and volcanic seamounts then show positive anomalies.

(Luis, 2007) using the multibeam topography grid (Figure 6a). These reductions remove predictable effects of field skewness and topographic relief and produce a mapping of the magnetization variation at the seafloor assuming a uniform source layer thickness (1 km).

2.5. IMI-30 Deep-Towed Side Scan Sonar Data

The IMI-30 deep-towed side scan sonar vehicle (Edwards et al., 2006; Rognstad et al., 2003) was deployed in the SEMFR area and towed at a nominal altitude of ~500 m above the seafloor and tow speed of 1–2 knots. The sonar side scan swaths have a width of up to 5 km, across-track resolution of 0.3–3 m, and long-track resolution of 0.6–3 m depending on vehicle speed and ping rate (Edwards et al., 2006). The tracks were oriented primarily along the forearc slope and included parts of the Fina Nagu Volcanic Chain (FNVC) at

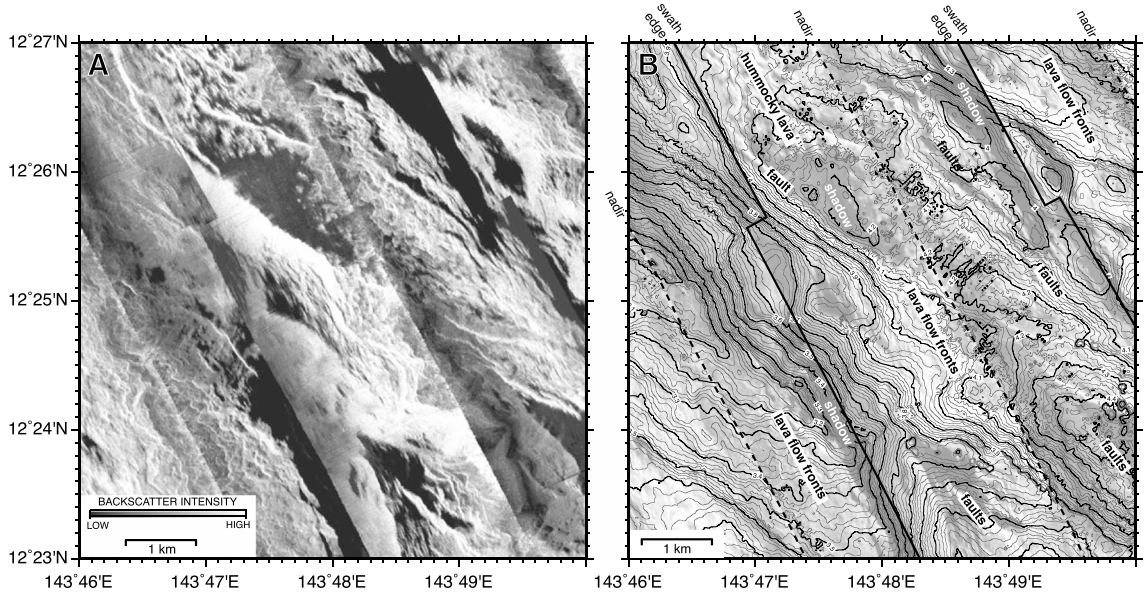

Figure 7. IMI-30 side scan sonar detail. (a) Sonar backscatter imagery with high intensities shown in lighter shades of gray and low intensities and shadows are dark. (b) Interpreted geology superimposed on a muted side scan image with 20 m bathymetry contours from the R/V *Thompson* EM302 multibeam sonar. The IMI-30 track nadirs are indicated with dashed lines and swath edges with solid lines. The tow vehicle was flown at a nominal altitude of 500 m above the seafloor. The data show closely spaced faults and local lava flows with no continuous volcanic axis. Similar terrain characterizes broad areas of the southern Mariana margin. The full side scan mosaic and EM302 multibeam bathymetry maps are shown in Figures S1 and S2, respectively.

the shallow end to near the 6,000 m depth limit of the vehicle toward the trench. The tracks were spaced at approximately 2 nautical miles (~3.7 km), which afforded complete nominal swath coverage of the survey area although high seafloor relief created frequent acoustic shadows. The area of the IMI-30 survey in SEMFR is shown in Figure 2 on the regional multibeam map. The complete side scan mosaic is shown in Figure S1 along with the corresponding hull-mounted R/V *Thompson* EM302 multibeam data in Figure S2. A detailed interpreted section of the IMI-30 side scan imagery showing characteristic features of the area is shown in Figure 7.

3. Results

We use the various data sets described above to examine the mode of extension and crustal accretion in the southern Mariana margin from various perspectives. Multibeam and side scan sonar data image seafloor fabric to examine the pattern of volcanic accretion and tectonic deformation across the area. Earthquake seismicity reflects the distribution and pattern of current tectonic deformation. Magnetic data are used to assess the organization of crustal accretion into narrow or diffuse zones. Gravity data reflect crustal thickness variations. We also summarize relevant previous measurements of water content in erupted lavas and derive mantle water contents. These data indicate distinct "diffuse" and "focused" modes of extension and crustal accretion in the southern Mariana margin that appear to be mediated by mantle water content.

3.1. Seafloor Fabric in the Southern Mariana Margin

The southern Mariana margin has only thin sediment cover so that multibeam bathymetric mapping can directly image most of the basement fabric formed by volcanic crustal accretion and tectonic deformation. This part of the margin is shallower and has thicker crust inferred from gravity data (Kitada et al., 2006) (average depth = 3,517 m; crustal thickness = ~6.3 km) than the central Mariana Trough to the north (average depth = 3,858 m; crustal thickness = ~4.9 km), which suggests enhanced magma supply toward the south. The reason for the greater magmatic productivity here compared to the Mariana Trough to the north likely reflects a more hydrous mantle that experiences greater extents of melting, in proportion to the mantle water content, due to a lower solidus temperature (Stolper & Newman, 1994). Enhanced crustal thickness due to

inferred effects of elevated mantle water on melting is also seen in the Lau (Dunn & Martinez, 2011; Eason & Dunn, 2015; Martinez et al., 2006) and other backarc basins (Martinez & Taylor, 2003; Taylor & Martinez, 2003). South of 14°22′N, the slab lies directly beneath the backarc spreading axis, facilitating its hydration, whereas to the north the slab dips more steeply and is located east of the spreading center (Kitada et al., 2006). The two flanks of the southern Mariana margin have distinct basement fabric trends (Martinez et al., 2000) separated by the backarc seafloor spreading center, the MGR, and its westward continuation, the DSZ (Figure 2). The northern flank fabric domain on the Philippine Sea plate conforms with the shape of the MGR/DSZ axis and appears to passively record the crustal fabric from the West Mariana Ridge, the rifted remnant arc, to the present zones of accretion on the MGR/DSZ. There are second-order differences in the character of the crust accreted on the MGR versus DSZ, however. Ridge-like topographic features flanking the MGR may represent abyssal hill-type fabric, although some of the more prominent ridges may have formed by ridge jumps or rapid ridge propagation events (e.g., Perram et al., 1993) that caused ridge axes to be cut off and abandoned on the Philippine Sea plate (Seama & Okino, 2015). Discontinuities and changes in trend between sets of these lineated ridges are probably nontransform ridge segmentation boundaries. Thus, the fabric flanking the MGR on the Philippine Sea plate is consistent with seafloor spreading fabric formed on a magmatically robust ridge that became part of the rigid Philippine Sea plate as it spread from the axis and was not further deformed.

The narrow seafloor spreading axis of the MGR ends near 143°13′E and is replaced by the broader DSZ of crustal accretion extending westward to the Southwest Mariana Rift (SWMR), which has undergone much less opening and is in a tectonic rifting stage. The basement fabric on the northern flank of the DSZ displays similar trends to the MGR flanks but has several distinctive features. A high backscatter zone indicating recent volcanism is tens of kilometers wide. Both the zone of active volcanism and the flanking area on the Philippine Sea plate have numerous small seamounts, only the larger of which are indicated in Figure 2b. In contrast, the crust flanking the MGR on the Philippine Sea plate has almost no individual seamounts. The crust flanking the DSZ on the Philippine Sea plate has a finely lineated tectono-volcanic fabric trending subparallel to the overall trend of the DSZ, which is distinct from the larger and more widely spaced abyssal-hill-type fabric flanking the MGR. Thus, on the Philippine Sea flank of the margin, the basement trends are subparallel to the extensional zones but differ in character between the MGR and DSZ.

South of the MGR/DSZ, fabric in the southern Mariana Platelet has an entirely different character. Basement lineations trend at variable but high angles to both the MGR/DSZ and the trench. There are no lineations subparallel to the trend of the spreading axis except within about 5 km of the MGR axial high, and the transition to the high-angle fabric is abrupt. A similar abrupt transition in basement fabric occurs south of the DSZ (Figure 2). The lineations shown in Figure 2b were traced from the larger offsets and only outline the main trends in the area; in detail seafloor fabric is much more finely lineated forming a pervasive pattern of closely spaced and anastomosing faults and fissures that trend subparallel to the indicated lineations (Figures S1 and S2). Faults are larger in the eastern part of the margin and toward the trench where they form deep rift valleys along the inner trench slope of the SEMFR (Ribeiro, Stern, Kelley, et al., 2013).

To the south of the DSZ on the Mariana platelet, there are no small seamounts and the fabric is oriented at a high angle to the trend of the DSZ, similar to the southern flank of the MGR but the azimuths broadly curve maintaining a roughly orthogonal orientation to the trend of the MGR/DSZ. Whereas the southern flank of the DSZ has no small seamounts, the southern flank of the MGR has two groups of large seamounts. One is the Fina-Nagu volcanic chain (FNVC) located 30–40 km from the MGR (Brounce et al., 2016). The second group consists of the Toto caldera (Gamo et al., 2004) and several smaller seamounts closer to the axis of the MGR (referred to as the Patgon-Masala Volcanic Chain by Masuda & Fryer, 2015). Both groups have been described as arc front-type volcanoes (Brounce et al., 2016; Masuda & Fryer, 2015). The seamounts of the FNVC form an unusually closely spaced alignment of volcanic cones and calderas that trend NNE-SSW, subparallel to the MGR (Figure 2). The flanks of the volcanoes overlap rather than forming the distinct spaced edifices more typical of the arc volcanic front. They appear to be faulted by the same extensional stresses forming the fabric at high angle to the spreading center. Along the FNVC, the breached caldera walls, tectonized volcano flanks, and low backscatter suggest limited recent volcanic activity. The FNVC edifices are more conical and less faulted toward the NE, suggesting an age progression with younger edifices to the NE (Brounce et al., 2016). The second set of volcanic edifices, proximal to the MGR, are less faulted in general and possibly younger than the FNVC (Masuda & Fryer, 2015).

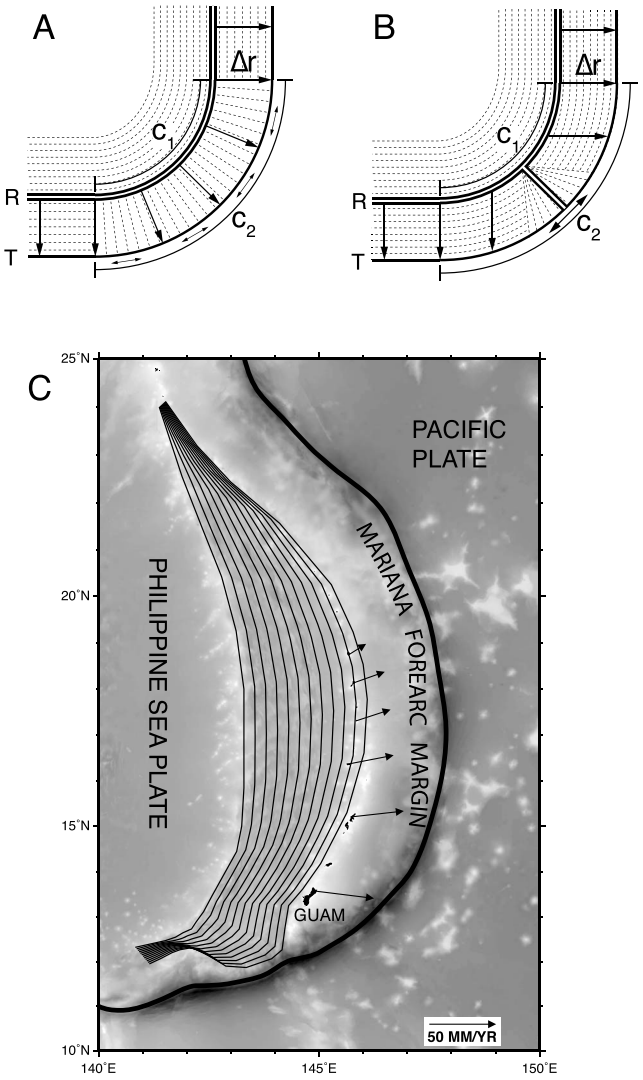

Figure 8. Schematic diagrams illustrating idealized components of extension in backarc basins. (a) Diffuse tangential extension of the margin due to a curving trench undergoing rollback. Trench rollback occurs perpendicular to the trend of the trench so that in the curved section the change in length of the trench ($\Delta C = C_2 - C_1$) is given by $\Delta C = \pi/2 * \Delta r$, where Δr is the change in radius of curvature due to rollback. (b) Curving trench with components of extension taken up along an organized spreading center with no diffuse deformation of the margin. The trench rolls back in two orthogonal directions, and the divergence is taken up at a triple junction on organized seafloor spreading centers. Basement fabric conforms with the geometry of the seafloor spreading axes. In Figures 8a and 8b spreading centers are indicated by double lines (labeled R) and trenches by single bold lines (labeled T). Rollback is indicated by single arrows and tangential extension by double arrows. Trench curvature is idealized as a circular quarter sector separating linear trench segments. (c) The gray shade bathymetry map of the Mariana area with inferred opening geometry schematically depicted as fine lines showing successive steps in the opening of the backarc basin. The heavy line is the trench. The arrows are geodetic vectors from Kato et al. (2003) with respect to the Philippine Sea plate. In the central Mariana forearc north of Guam broadly distributed tangential extension occurs due to trench-normal rollback as in Figure 8a. In the margin SW of Guam the wide Eocene-Miocene forearc itself rifted apart resulting in diffuse magmatic accretion over the slab to near the trench instead of forming an organized spreading axis as in Figure 8b.

3.2. Mantle Water Content Beneath the Southern Mariana Margin

Of the samples from the MGR and DSZ reported by Brounce et al. (2014), five erupted at sufficiently high pressure that they are likely to have erupted undersaturated with respect to H_2O (i.e., H_2O is unlikely to have degassed) and thus retain some record of the water contents of their mantle sources. Four of these samples are wax cores from the MGR, and one is a dredge sample from a seamount in the DSZ (13D). We followed the methods of correction for fractional crystallization for Mariana Trough basalts reported by Kelley et al. (2010) and summarize the procedure here. We reconstruct the primary melt compositions in equilibrium with mantle olivine (i.e., 90% forsterite composition, or Fo90) by first tracing the major element compositions of the five samples that are likely to be undersaturated with H_2O back to MgO = 7.1 wt % along the previously determined liquid line of descent for Mariana Trough basalts with >1.5 wt % H_2O, then adding olivine in 0.1% increments until Fo90 equilibrium is reached. This reconstruction reveals that primary MGR melts (i.e., melts in equilibrium with their mantle sources) have ~1.4–1.6 wt % H_2O and 0.72–0.86 wt % TiO_2. Similarly, the primary melt at the DSZ seamount has ~1.4 wt % H_2O but a lower TiO_2 (0.56 wt %). Using TiO_2 as a proxy for melt fraction (e.g., Kelley et al., 2006; Kelley et al., 2010; Stolper & Newman, 1994), and adopting assumptions about partition coefficients and source composition from Kelley et al. (2010), the MGR magmas suggest mantle source H_2O contents of 0.19–0.25 wt %. This is the high end of the range previously reported for backarc basin basalts (BABs) of the Mariana Trough north of the MGR (Kelley et al., 2010), although the previously studied samples appear randomly distributed along the length of the spreading axis and there is no geographically distinct "wet spot" in the Mariana Trough other than the MGR. Likewise, the melt fractions beneath the MGR suggested by primary melt TiO_2 contents range from 12 to 15%, which is also at the high end of the Mariana Trough BAB range. The DSZ seamount, on the other hand, indicates an unusually high source H_2O content of 0.3 wt %, and a melt fraction of 21%, both of which are more typical of arc-front volcanoes in the Marianas (Kelley et al., 2010). Collectively, these observations suggest a distributed zone of regionally elevated mantle H_2O contents and higher extents of mantle melting than characterize the rest of the Mariana Trough.

3.3. Earthquake Seismicity and Kinematics of the Southern Mariana Margin

Figure 3 shows focal mechanisms from the Global Centroid Moment Tensor Project (Dziewonski et al., 1981; Ekström et al., 2012) for the Mariana Trough. *P*-axis azimuths (indicated by red bars) show that motion on thrust events (red focal mechanisms) is mostly directed nearly orthogonally to the trench regardless of the motion of the incoming Pacific plate (shown as small circles of Pacific-Philippine Sea plate motion following the Euler pole of Kato et al., 2003). We infer from this pattern that the *p*-axes of teleseismic thrust events reflect the trench normal component of motion and thus parallel the rollback direction of the slab as predicted from kinematic arguments (Figure 8a) (e.g., Dewey, 1980). Trench-normal *p*-axis azimuths of thrust events also characterize the New Hebrides subduction zone, which also has an actively opening backarc basin, and a pronounced ~90° curvature of

the trench (Patriat et al., 2015; Pelletier et al., 1998). The curving Mariana and New Hebrides trenches imply some oblique convergence as the larger subducting plates have fairly uniform directions of motion across these trenches. In the New Hebrides system, strike-slip faults or zones develop inboard of the trench and take up the strike-slip component so that convergence and *p*-axis azimuths remain normal to the trench (Patriat et al., 2015). In the southern Mariana Trench, the strike-slip component is apparently taken up at the trench and subduction interface itself, as no strike-slip faults and very few strike-slip focal mechanisms are observed in the upper plate. Thus, along the Mariana Trench the rollback direction is approximately orthogonal to the trench and curves by over 90° from north to south (Figure 3) and generates trench-normal *p*-axis azimuths despite oblique motion along the southern margin, implying that the strike-slip component is relieved aseismically. The distribution of thrust events can also be used to estimate the subduction interface area between upper plate and slab and is shown as a purple dashed line in Figure 4. We interpret the area between the trench (yellow front symbols) and the purple dashed line, which forms the basinward limit of thrust events, as underlain by the subduction interface.

In agreement with the indicated rollback direction from the *p*-axis azimuths, the *t*-axis azimuths of extensional and strike-slip events in the basin are generally subparallel to and follow the changing normal direction of the curving trench from north to south (Figure 3). An exception occurs in the southern Mariana margin, however (Figure 4). Whereas the *p*-axis azimuths continue to generally trend orthogonal to the trench, between ~143°E and 144° 20′E, the *t*-axis azimuths are oriented subparallel to the trench. This orientation is roughly orthogonal to local basement fabric trends (Figure 2b) but is not parallel to the GPS opening vector at Guam with respect to the Philippine Sea plate (Figure 4; Kato et al., 2003). This suggests that the eastward motion of the forearc margin near Guam relative to the Philippine Sea plate is not the only control on the extension in the margin to the south. In the southern margin the *t*-axis azimuths broadly parallel the changing trend of the spreading axis in this area and indicate a nearly orthogonal component of extension to the ridge axis. We interpret the pattern of *p*- and *t*-axis azimuths as reflecting distinct modes of strain along the southern margin. Along the subduction interface, thrust events dominate and are directed nearly orthogonally to the trend of the trench, despite the highly oblique relative motion between the Pacific and Mariana platelet (Figure 3). This implies weak coupling along the subduction interface so that the nearly E-W relative motion of the Pacific plate at the SW end of the trench does not influence the seismicity, and thrust events reflect the trench normal rollback component of the subduction interface. Within the southern Mariana platelet, *t*-axis azimuths of normal and strike-slip events primarily reflect extension due to the relative ~E-W opening of the forearc and a secondary component of southward flow of material to fill in the forearc rift. The ~N-S component of this extension is taken up primarily at the MGR/DSZ, which curve to an ~E-W orientation and are magmatically robust, producing few teleseismic events.

The rifting and breakup of the southern Eocene-Miocene forearc create a localized gap (Figure 8c), unlike the broad tangential extension of the central Mariana forearc that is accommodated by distributed tectonic extension of the preexisting material (Figure 8a) apparently without new crustal accretion (Wessel et al., 1994). In the southern Mariana margin the preexisting wide (~150 km) and thick Eocene-Miocene forearc lithosphere ruptured and separated by relative eastward motion of the Santa Rosa Bank forearc block and Guam away from the conjugate forearc to the west. This expanding gap induced the advection of new asthenosphere to flow above the slab and toward the trench (Figure 8c). The influx of new material and accretion of new crust could have been accommodated by the formation of an organized spreading center in triple junction configurations with the MGR to the north and with the trench to the south (Figure 8b), but there is no indication in the magnetics or basement fabric that this ever happened. Instead, the influx of new asthenosphere and accretion of new crust appears to have been broadly distributed across the widening gap, as it is at present.

Almost all earthquakes large enough to have teleseismic focal mechanism solutions plus most ISC events (Figure 3, green dots) occur within the Mariana platelet. In comparison, very few teleseismic events occur north and west of the spreading axis on the Philippine Sea plate proper. The distribution of earthquakes within the Mariana platelet indicates broadly distributed active extension. Active tectonic extension subparallel to the trench and spreading center occur from ~143°E to 144°20′E and scattered approximately trench normal extensional events continue eastward within a broad zone to ~142°20′E. Thus, the southern Mariana platelet within an ~200 km wide zone is actively extending. At the western end of this zone tectonic extension focuses to the Southwest Mariana Rift (SWMR) and the extensional direction indicated by the *t*-axis

azimuths within the rift is subparallel to the southerly directed *p*-axis azimuths of the thrust events at the subduction interface (Figure 4).

The diffusely distributed deformation of the southern Mariana margin is distinct from other near-trench settings, such as at the northeastern end of the Tonga Trench (Wright et al., 2000) and southern end of the New Hebrides trench (Patriat et al., 2015), where well-organized (narrow plate boundary zone) spreading centers intersect the trench and take up trench-parallel extension. In these settings, the divergent axes are located behind the arc volcanic front and there is little to no slab underlying the spreading centers, which may affect the degree of hydration of the lithosphere and therefore lead to a stronger lithosphere and more rigid plate-like behavior. Another setting where limited hydration may affect plate boundary behavior is within backarc basin interiors distal from the trench. For example, in the North Fiji Basin, the curving New Hebrides trench leads to diverging rollback directions (Patriat et al., 2015) but narrow plate boundary zone triple junctions form in the plate interior (Auzende et al., 1994; Lafoy et al., 1990) (Figure 8b).

3.4. Gravity Anomalies of the Southern Mariana Margin

The mantle Bouguer anomaly (MBA; Figure 5) was calculated following standard procedures used at mid-ocean ridges (Kuo & Forsyth, 1988) using satellite-derived free air gravity anomalies (Sandwell et al., 2014) and the compiled multibeam bathymetry grid (Figure 2). To summarize, this removes the gravity effect of the water/seafloor interface and of the crust/mantle interface assuming a crust with constant thickness (6 km). Remaining anomalies reflect departures from these assumptions. We show the color-coded MBA of the southern margin in Figure 5 with superimposed 250 m bathymetry contours for reference. We examine the MBA to assess crustal thickness changes, although in convergent margin settings the MBA displays several prominent effects due to other causes. The pronounced step in values across the trench (Figure 5, green dashed line) between the Mariana margin and Pacific plate is mostly due to lithospheric age contrast rather than crustal thickness changes. Pacific plate oceanic crust is deeper and has generally higher MBA values than Mariana margin crust because it is part of an older, cooler, and thicker lithosphere that has subsided. Some of the gravity variation associated with volcanic seamounts on the Pacific plate is evident (reddish areas), but as we are primarily interested in the margin values, we allow values on the Pacific plate to saturate and so appear white. As noted above, we have also not removed slab gravity effects as these are predicted to be small and have long wavelengths (Watts & Talwani, 1975) compared to crustal sources. In addition, the slab is continuous beneath this area and has only broad variations (as determined from Benioff zone seismicity (Hayes et al., 2012) so should have a similar effect in rifted and unrifted forearc areas. Thus, we interpret the main variation in Figure 5 (the $>$150 mGal red to purple color range) as due to the rupturing of the pre-existing Eocene-Miocene forearc (labeled Mariana Ridge) replacing older and thicker crust with much thinner newly accreted crust (in the area labeled "forearc rift"). We interpret a secondary anomaly as due to nonisostatic support of the outer forearc where the slab and upper plate lithosphere are in contact. We estimate the region of nonisostatic support of the outer forearc (between the green and purple dashed lines in Figure 5) from the band of thrust earthquakes (Figure 4) that we infer are associated with the subduction interface. Based on an analysis of the Tonga forearc, which has a simpler linear geometry (see Figure 1 in Martinez & Taylor, 2002), we estimate that the nonisostatic support of the outer forearc may increase gravity by $<$50 mGal. Remaining systematic anomalies form broadly decreasing values varying by $<$100 mGal from the outer forearc high to the West Mariana Ridge. Smaller variations of $<$50 mGal (orange to green color scale) are likely due to crustal thickness variations within the basin. Another contribution to the MBA gravity high along the outer forearc is a change in lithology that characterizes the outer slope. Much of the outer slope of the Mariana forearc exposes deep forearc crustal sections (Reagan et al., 2013) and mantle peridotite (Bloomer & Hawkins, 1983; Ohara & Ishii, 1998), especially at depths $>$5,800 m. Changing lithologies and densities depart from the uniform thickness and crustal density assumption of the MBA.

Inboard from the outer margin topographic highs, the seafloor is flatter and deeper and is underlain by strike-slip and normal earthquakes rather than thrust events (Figure 4). We infer that this part of the margin is in local isostatic equilibrium with the underlying mantle wedge asthenosphere and no longer rests on the slab. This part of the Mariana platelet is generally a few hundred meters deeper (~500 m) than the corresponding Philippine Sea flank. This depth difference isostatically predicts about a 1,900 m thinner crust for the Mariana platelet side relative to the Philippine Sea flank. A simple one-dimensional estimate of the expected Bouguer gravity change due to the isostatically predicted change in crustal thickness yields ~35 mGal, whereas the

observed difference in MBA gravity is ~47 mGal. The 12 mGal discrepancy may be at least partly due to poorly constrained slab gravity effects. The difference in depth between the two flanks may be due to an original asymmetry in crustal thickness or to postaccretion stretching of the Mariana Platelet crust. Alternatively, the deeper seafloor on the Mariana Platelet side relative to the Philippine Sea flank may be due to a dynamic effect (Billen & Gurnis, 2001) involving weak coupling of the low-viscosity mantle wedge to the subducting slab in this area.

The MBA and depth variations indicate large changes in crustal thickness along the forearc. MBA values are ~150 mGal higher (red to pink areas) in the rifted forearc than along the unrifted parts of the Mariana Ridge to the west and east (blue to purple areas) indicating much thinner crust at comparable distances from the trench (Figure 5). The observed differences in MBA gravity are consistent with much thicker crustal roots beneath the unrifted Mariana Ridge forearc than beneath the rifted forearc. Near the central Mariana margin, the crustal thickness of the submerged Eocene-Miocene forearc has been seismically estimated to be 21 km (Calvert et al., 2008) and is probably at least that thick around the higher-standing forearc blocks including Guam of the southern Mariana Ridge. Broadly, the southern Mariana basin crust has been estimated from gravity data to be on average about 6–7 km thick (Kitada et al., 2006) and our local analysis suggests possibly a 1.7 km thinner crust on the Mariana platelet compared to the Philippine Sea flank of the margin. The forearc crust may thus have thinned from the ~21 km crustal thicknesses that characterize the Eocene-Miocene forearc in the Central Mariana area to 0–5 km in the southern basin forearc gravity high shown in Figure 5. This thinning was achieved by rifting apart the preexisting Eocene-Miocene forearc so that the present-day crustal thickness in the basin represents predominantly newly accreted volcanic material. High-standing blocks along the outer forearc high may, however, represent remnant rifted blocks of the Eocene-Miocene forearc although apparently recent basaltic volcaniclastics have been recovered even along the outer trench slope (Stern et al., 2014). Ages of sampled volcanic material in the SEMFR area range from about 2.7–3.7 Ma (Ribeiro, Stern, Kelley, et al., 2013). At current opening rates of about 45 mm/yr determined geodetically on Guam (Kato et al., 2003) and magnetically on the MGR (Seama & Okino, 2015), the present ~200 km width of the southern basin between Guam and the West Mariana Ridge could have formed in about 4.5 Myr. However, at Guam this rate represents the trench-normal component of opening. Along the southern margin trench-parallel extension adds another component of opening (Figure 8) not reflected in the GPS rates, and the rupture of the wide Eocene-Miocene forearc may have additionally resulted in flow of new margin material toward the trench so that the overall southern forearc extension rates are likely greater.

3.5. Magnetic Anomalies of the Southern Mariana Margin

Despite complex and high relief basement (Figure 6a), the SEMFR area has sufficiently dense sea-surface magnetic anomaly data (typical line spacing $<$5 km) to constrain the three-dimensional field (Figure 6b). The total field anomaly does not show evidence of lineated magnetic anomalies. Instead, anomalies form broad blob-like variations (Figure 6b). In order to examine the magnetic character of the area further, we removed predictable distorting effects as described above. The reduced-to-the-pole anomaly shows positive values over the FNVC edifices, the MGR spreading center and the adjacent Toto caldera as well as a possible linear magnetic stripe to the east of the MGR axis near the northern edge of the map (Figure 6c). A further inversion for seafloor magnetization was carried out, which accounts for topographic effects and predicts the source layer magnetization strength assuming that it has a uniform 1 km thickness (Figure 6d). This reduction further reinforces the positive values associated with the MGR spreading center, the adjacent Toto caldera and FNVC. The Mariana platelet has generally negative magnetizations that are mostly weak (~ $-$5 A/m) but become somewhat more negative (~ $-$10 A/m) in the area adjacent to the Santa Rosa Bank (NE edge of Figure 7a). Low-amplitude (~5 A/m) positive magnetizations are associated with the outer forearc highs (near SW edge of Figure 6a). Predominantly, low-amplitude negative magnetizations (~ $-$5 A/m) are associated with the SEMFR.

The overall character of the magnetic anomalies and seafloor magnetization of the southern margin do not support organized seafloor spreading as the formative process. Although distinct positive anomalies are locally associated with the MGR spreading center and the nearby large volcanic edifices, most of the southern Mariana platelet has weak, broad, and irregular patches of magnetic variation inconsistent with a progressive formation from a focused axis. The low magnetization strength suggests a nonfocused or distributed manner of crustal accretion over an extended period of time such that volcanic emplacements of mixed polarity

(spanning magnetic reversals) occurred within the same area. This could account for a magnetic source layer with a normal or excess thickness yet weak net magnetization. Given the variable and complex basement fabric trends, it is also possible that crustal blocks have rotated, which would also affect the magnetization solution as this effect is not accounted for in the inversion. Because of an inherent uncertainty in magnetization reductions expressed by the "annihilator" solution (a theoretical magnetization distribution for the given seafloor bathymetry that produces no change in the observed field) (Parker & Huestis, 1974), the interpretation of low-amplitude variations are particularly suspect. Despite these complications, we suggest that the overall character of the magnetic anomalies and of the various reductions do not support crustal formation within the forearc rift by an organized seafloor spreading center.

3.6. SEMFR IMI-30 Side Scan Sonar Survey

The IMI-30 side scan sonar survey in the SEMFR area does not show typical seafloor spreading structure (Figure S1). Fault trends are variable and closely spaced with superimposed crisscrossing patterns suggesting different generations of faults formed under different stress directions. The finely spaced faults (often $<$1 km apart; Figure 8) indicate a weak lithosphere that cannot form large fault blocks. Near the southern SEMFR survey (~143°52′E, 12°15′N; Figure S1), two prominent fault trends are oriented at high angles to one another. This tectonic morphology contrasts with the subparallel, more widely spaced abyssal hill faults typically formed through organized seafloor spreading (e.g., Goff, 1991). Volcanic constructions appear to be emplaced through scattered small local effusion sites (Figure 7) without a central axis. The volcanic morphologies show a mixture of smooth sheet flows and hummocky mounds in close proximity (Figure 7), suggesting variable effusion rates at different times. Backscatter is high throughout the area surveyed (Figure S1), and regional shallow-towed side scan sonar surveys indicate high backscatter throughout the southern margin well beyond the area of the IMI-30 survey (Fryer et al., 2003). This pattern is inconsistent with organized seafloor spreading, where backscatter intensity decreases away from a focused neovolcanic zone due to sediment accumulation on the ridge flanks with age, as occurs on the MGR flanks west of Guam (Hagen et al., 1992). The seafloor volcanic and tectonic morphologies indicate a diffuse accretion pattern with superimposed generations of individually small volcanic emplacements and variably oriented faults.

4. Discussion

Trench-parallel rifting and breakup of the predecessor Eocene-Miocene southern Mariana forearc and ongoing opening of the margin allow us to examine how new oceanic crust and lithosphere form over an actively subducting slab. Detailed geophysical surveys together with regional data reveal contrasting "rigid plate" and "diffuse" styles of volcano-tectonic deformation between the two flanks of the southern Mariana margin. Below we describe a model for this difference in behavior between the two flanks of the southern Mariana margin and discuss implications of this model for subduction zone infancy and for what enables the narrow divergent plate boundary zones of plate tectonics in general.

4.1. Distinct Styles of Crustal Accretion and Deformation in the Southern Mariana Margin

The NW flank of the MGR/DSZ on the Philippine Sea plate behaves as rigid lithosphere recording the tectonic and volcanic fabric formed when the crust was accreted, undergoing little if any subsequent deformation once outside the plate boundary zone. This is shown by basement fabric, which conforms with the shape of the spreading axes, the paucity of teleseismic earthquake activity, and the occurrence of apparent linear magnetic isochrons recorded on the Philippine Sea flank of the MGR (Seama & Okino, 2015), although available data do not sufficiently resolve the magnetic character of the DSZ flank. In addition, regional geodetic data indicate a coherently rotating Philippine Sea plate with a well-defined Euler pole (Kato et al., 2003). These characteristics are typical of oceanic crust and lithosphere formed by organized seafloor spreading along narrow plate boundary zones.

In contrast, the Mariana platelet south and east of the MGR and DSZ has very different characteristics. Volcano-tectonic fabric is oriented at high angles to the trend of the MGR/DSZ indicating that the crust was either not formed on these systems or strongly deformed soon after formation. Teleseismic earthquakes are abundant and distributed throughout the southern Mariana platelet (Figure 4). Geodetic measurements within the Mariana platelet from Agrihan (18°44′N) to Guam (13°34′N) determine southward increasing rollback velocities relative to the Philippine Sea plate and internal deformation of the platelet (Kato et al., 2003).

Although there are no geodetic measurements in the entirely submarine margin SW of Guam, focal mechanism *p*-axis azimuths corroborate continuing trench-perpendicular rollback in the southern margin even as the trench curves by >90° overall. Within the central and northern Mariana platelet, teleseismic earthquake *t*-axis azimuths are generally subparallel to the *p*-axes, indicating primarily radial extension subparallel to the rollback direction and clustered near the spreading centers (Figure 3). Trench-parallel extension due to trench-perpendicular rollback along the broad arc of the central and northern Mariana trench (Figure 8a) may account for broadly distributed deformation of the forearc (Karig et al., 1978; Stern & Smoot, 1998; Wessel et al., 1994) but the main component of extension remains trench-perpendicular. In the southern margin, however, extensional *t*-axis azimuths within a wide swath of the southern Mariana platelet are oriented nearly orthogonally to the thrust *p*-axis azimuths near the trench (Figure 4), indicating a significant ~E-W component of extension.

This large ~E-W component of extension is likely due to the complete rupturing of the preexisting Eocene-Miocene forearc in the southern margin that separated a significant thickness and width (~150 km) of cold forearc lithosphere, inducing trenchward advection of hot mantle wedge asthenosphere to fill this void (Figure 8c). The main extension is caused by the thick, old forearc block including the Santa Rosa Bank and Guam moving eastward subparallel to the trench and away from the conjugate old forearc of the SW end of the Mariana Ridge (Figure 8c), as indicated by geodetic data (Kato et al., 2003). Along the central and northern Mariana margin, the forearc is about 175–180 km wide and the seismically identified crust averages about 20 km thick (Calvert et al., 2008), with a potentially thicker mantle lithosphere beneath. The rupture and separation of a similar block of lithosphere along the southern forearc would have caused flow of a large volume of mantle wedge asthenosphere to fill the void extending to the trench (Figure 8c). The present southern margin forms a bowed-out shape in this area (Figure 2), extending the trench farther seaward than adjacent to the remaining unrifted parts of the forearc margin. This suggests that the new material filling the forearc rift is thin and weak lithosphere that gravitationally flowed farther out over the slab than the bordering thicker and stronger lithosphere of the unrifted cold and old forearc. The pervasive basement volcanotectonic fabric of much of the rifted forearc area indicates a diffuse deformation of the new margin material consistent with a thin and weak southern Mariana margin lithosphere possibly embedding a few stronger remnant forearc blocks along its outer edge (Figure 2). The rupturing of the southern forearc margin and relative eastward rollback of the overall Mariana trench and forearc may be due to the regional westward trench advance of the entire IBM system (Carlson & Mortera-Gutiérrez, 1990) and possible outflow of asthenosphere from beneath the Philippine Sea plate (Ribeiro et al., 2017).

4.2. Southern Mariana Platelet Magmatism

Slab contours derived from Wadati-Benioff zone seismicity (Hayes et al., 2012) show that the entire southern Mariana platelet in the study area is underlain by the subducting slab (Figure S3). Despite shallow slab (<100 km) depths beneath the Mariana platelet, ^{40}Ar-^{39}Ar ages date young volcanics (2.7–3.7 Ma) within the SEMFR area in the SE part of the southern margin (Ribeiro, Stern, Kelley, et al., 2013). These samples document new volcanism indicating that above-solidus thermal conditions extended unusually close to the trench. SEMFR basalts have significant enrichments in slab-derived fluid-mobile elements (Ribeiro, Stern, Martinez, et al., 2013) and high water contents (~2%) (Ribeiro et al., 2015), indicating a hydrous mantle source, especially in light of evidence of significant water degassing (Brounce et al., 2016). Thus, as thick and cold preexisting forearc lithosphere was rifted apart, the void was filled with hot upwelling mantle wedge asthenosphere infused with water from the slab that underwent both pressure-release and hydrous flux melting. Slab motion induced mantle corner flow, and westward trench advance with respect to Eurasia (Kato et al., 2003) may have also helped to bring hot mantle wedge asthenosphere to near the trench axis (Ribeiro et al., 2017).

The age distribution of basaltic rock samples suggests younger volcanism away from the trench (Ribeiro, Stern, Kelley, et al., 2013), but dated samples are too few to be definitive. Nevertheless, this trend is expected based on general considerations. As the forearc rift initiated, the area undergoing extension would have been narrower than at present, thereby inducing more rapid mantle upwelling to fill the void and inducing corresponding vigorous pressure release melting and volcanism. Unlike mid-ocean ridges, however, the zone of crustal accretion did not focus to a narrow plate boundary zone (Figure 9). This is demonstrated today by the broadly distributed pattern of extensional teleseismic earthquakes across the southern Mariana

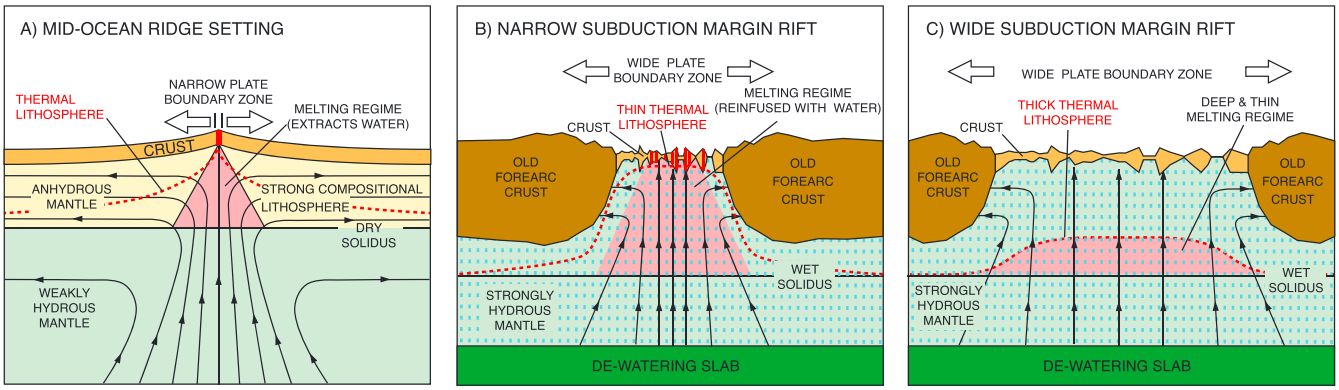

Figure 9. Model of the effects of water on mid-oceanic and convergent margin lithosphere. (a) At mid-ocean ridges the mantle is weakly hydrous and mantle melting in the subaxial melting regime (pink area) dehydrates the residual lithosphere (yellow area) causing an increase in viscosity of 2 orders of magnitude or more (Hirth & Kohlstedt, 1996). This creates an anhydrous "compositional lithosphere" that may help to focus melt and deformation to the narrow plate boundary zones characteristic of oceanic spreading centers (Phipps Morgan, 1997). The compositional lithosphere is further strengthened by cooling with time creating a thickening thermal lithosphere (above red dashed line) on the ridge flanks (e.g., Parsons & Sclater, 1977). (b) Schematic ~E-W vertical cross sections through the southern Mariana convergent margin above the subducting slab (dark green area). When the margin rift was narrow vertical mantle advection rates were fast (indicated by closely spaced arrowed flowlines) between the rifted edges of the old Eocene-Miocene forearc (brown areas). The subducting slab provided a continuous flux of water (blue dashes) to the overlying mantle wedge (light green). Melting began at the wet solidus but because of the continual addition of new slab-derived water, mantle dehydration could not occur. The mantle remained hydrous and weak and the thermal lithosphere was thin due to rapid vertical mantle advection rates and tectonic deformation and volcanism were broadly distributed. (c) As opening continued and the rift widened, vertical mantle advection rates proportionately slowed (indicated by more widely spaced arrowed flowlines). The thermal lithosphere thickened by cooling greatly diminishing the size of the melting regime (pink area) and effectively shutting down volcanism at the seafloor. The mantle cooling also progressed from the trench toward the backarc spreading center and may have caused extinction of the Fina Nagu Volcanic Chain and displacement of arc volcanism toward the Malaguana-Gadao Ridge. Slab dewatering continued and mantle lithosphere throughout the margin remained hydrous and weak so that tectonic deformation remained broadly distributed, as shown by earthquake seismicity.

platelet indicating ongoing active distributed trench-parallel extension (Figure 4). Regional shallow-towed side scan sonar mapping (Fryer et al., 2003) also shows that the entire southern margin has high backscatter with no evidence of a localized axis. In addition, near-bottom side scan sonar data show a distributed pattern of volcanism (Figure 8) with no narrow neovolcanic zone (Figure S1). Volcanic flows and mounds occur in small patches a few square kilometers in area separated by faulted terrains (Figure 7). Magnetic anomalies in the southern platelet also indicate a diffuse manner of accretion with broad low-amplitude magnetic variations and no magnetic lineations (Figures 6b–6d). These data indicate a broad widening rift. For a widening rift, the rate of mantle upwelling decreases as the inverse of the width of the zone undergoing pure-shear extension (Buck et al., 1988). Thus, as the southern Mariana forearc rift widened, mantle upwelling rates decreased and cooling from both the slab and the surface would bring the mantle wedge to below-solidus temperatures (Figure 9). This cooling would be most efficient in the narrow nose of the mantle wedge near the trench and would progress inward from the trench. This expected pattern of cooling is consistent with the ages of volcanic rocks dated from the Mariana margin (Ribeiro, Stern, Kelley, et al., 2013) and suggests that by 2.7 Ma, much of the forearc margin mantle may have become too cold to sustain widespread active volcanism (Figure 9). Continuing extension and the identification of fresh-appearing volcaniclastics (Stern et al., 2014), however, suggest possible local areas of continuing volcanism within the broader region.

As the forearc wedge cooled, and only deeper and more trench-distal parts could sustain melting, an arc volcanic front may have begun to localize. Several factors may have influenced the initial development of an arc volcanic front. The widening rift would have resulted in a diminishing plate-driven component of mantle advection allowing hydrous flux melting to develop buoyant mantle diapirs. Buoyant diapirs of hydrous mantle could thus have initiated the FNVC, located today between 50 and 80 km above the slab (Figure S3). Continued upper plate extension would have displaced FNVC eruptive sites relative to diapiric magma sources linked to the slab perhaps accounting for the coalesced distribution of rifted volcanic edifices now present (Brounce et al., 2016), rather than the conical and spaced edifices that typically characterize the arc volcanic front. As mantle wedge cooling continued, however, even the mantle beneath the FNVC may have dropped below solidus conditions, accounting for the apparent paucity of volcanic activity and

highly tectonized appearance today of the volcanic complex. Arc front volcanism may have migrated further inward, now forming the Toto caldera and smaller edifices adjacent to the MGR (Masuda & Fryer, 2015) as an inchoate volcanic front. Arc melt also may be captured by the MGR itself (Becker et al., 2010), which is situated at ~80–100 km above the slab, a more typical loci for the arc volcanic front (Tatsumi, 1986).

4.3. The Southern Mariana Margin as an Analog for Subduction Zone Infancy

The tectono-magmatic development of forearcs remains poorly understood (e.g., Taylor, 1992) although these terrains are likely the formation sites of ophiolites, from which the structure and formation processes of oceanic crust are inferred (Stern et al., 2012; Stern & Bloomer, 1992). A distinctive aspect of subduction zone forearcs is the early, short-lived, and widely distributed (~300 km wide x up to thousands of kilometers long) contemporaneous volcanism that characterizes their formation (Arculus et al., 2015; Bloomer et al., 1995; Ishizuka et al., 2006; Stern & Bloomer, 1992; Taylor, 1992). A difficulty in understanding the processes that form these terrains is that subduction initiation is rare in the recent geologic record, and as noted by Taylor (1992) "There is no modern example of such extensive, contemporaneous, supra-subduction zone volcanism, which makes it one of the least understood aspects of the IBM system, and of the many ophiolites that have similar characteristics". Although the southern Mariana margin is not a nascent subduction zone, some of the processes involved in its formation and active today may have analogs to those inferred for subduction zone infancy. We explore these possible analogs below.

A common process that we deduce between subduction zone infancy and the present southern Mariana margin is lithospheric extension above a dewatering slab leading to new volcanic crustal accretion that includes what becomes the forearc. In models for the early IBM system, the first phase of this process involves spontaneous foundering of a lithospheric slab due to its gravitational instability (Stern & Bloomer, 1992). As this initial foundering is vertical it causes the edge of the foundering plate to pull away from the trailing plate in a form of trench rollback. The gap created is an extensional void filled by asthenospheric mantle flow that overrides the foundering and dewatering slab. Magmatism is induced by a combination of pressure release melting, as asthenosphere rises to fill the void, and hydrous flux melting from the dewatering slab (Reagan et al., 2010). As the slab continues to founder and the extensional zone widens, the volcanic products of this magmatism are not focused at a spreading axis but remain broadly distributed over a zone up to ~300 km wide (Stern & Bloomer, 1992; Taylor, 1992). This type of volcanisms lasts for 2–4 Myr before being replaced by more typical arc volcanic front edifices that form ~200 km from the trench (Ishizuka et al., 2006; Stern & Bloomer, 1992).

Although the two-dimensional conceptual model of Stern and Bloomer (1992) suggests that the early extension associated with slab foundering was directed perpendicular to the trench, in the actual IBM initiation, significant trench-parallel extension is additionally implied by evidence that the Central Basin Fault was active at the time of IBM subduction initiation (Deschamps & Lallemand, 2002). The Central Basin Fault was the active spreading center forming the West Philippine Basin at that time, which constituted the upper plate of the incipient subduction zone. The configuration of the Palau-Kyushu Ridge with respect to the Central Basin Fault and its associated magnetic isochrons extending across the West Philippine Plate (Deschamps & Lallemand, 2002) shows that the trend of the trench and opening within the upper plate were at high angles (Figure 1). Therefore, the early opening of the IBM system involved trench-parallel extension of the upper plate in addition to trench-normal rollback of the early slab, similar to the trench-parallel extension and trench rollback of the current southern Mariana margin.

The main difference between these two systems appears to be the lack of fluid mobile trace elements, suggesting little hydrous flux from the slab in the first-formed forearc basalts (FABs) in the IBM system (Reagan et al., 2010; Reagan et al., 2017) contrasting with the significant enrichment in fluid mobile elements and measured elevated water contents in the SEMFR volcanics (Ribeiro, Stern, Martinez, et al., 2013; Ribeiro et al., 2015). This difference may be explained by the fact that the current southern Mariana rifted margin formed over a preexisting long-lived subduction zone. Thus, pressure-temperature conditions for the full spectrum of slab dehydration and fluid transport mechanisms to the upper plate (diapirs, channels, grain boundary diffusion, etc.) were already in place and the preexisting mantle wedge was already hydrous as the current southern Mariana forearc rift formed. In the case of IBM subduction initiation these conditions and mechanisms did not exist and had to newly develop within a presumably MORB-source and weakly hydrous mantle. Thus, the composition of the early-formed FABs in the IBM system was MORB-like, lacking

strong slab fluid signatures (Reagan et al., 2010, 2017), whereas the SEMFR lavas have strong slab signatures and elevated measured water contents from their earliest stages (Ribeiro, Stern, Martinez, et al., 2013; Ribeiro et al., 2015). Whether the lack of slab fluid signature in the IBM FABs implies formation by organized seafloor spreading is not clear. The near synchronous ages of formation of the early volcanics of the IBM system across nearly 3,000 km along strike and 300 km across strike suggest a diffuse overall process (Ishizuka et al., 2006). However, it is also possible that there was early organized spreading on one or more spreading centers corresponding to the FAB eruption phase that was later supplanted by diffuse accretion of boninite and other volcanics as the mantle wedge became hydrous.

In any case, it appears that the bulk of the early volcanism that predates the localization of the IBM arc volcanic front formed in a diffuse manner over a wide zone (~300 km) (Ishizuka et al., 2006; Stern & Bloomer, 1992; Taylor, 1992). We infer that analogous processes are now active in the southern Mariana margin since the preexisting Eocene-Miocene forearc was rifted, triggering the formation of a new upper plate margin by distributed basaltic volcanism. At current opening rates determined geodetically at Guam (~45 mm/yr.; Kato et al., 2003), the present width of the basin between Guam and the West Mariana Ridge could be closed in ~4.5 Myr, which is broadly consistent with the age of the main phase of Mariana Trough magmatic spreading inferred in the central Trough beginning at ~5 Myr (Hussong & Uyeda, 1981). The trench-parallel rifting of the southern Mariana forearc probably began soon after that, and ^{40}Ar-^{39}Ar ages indicate volcanic emplacement ages of 3.7–2.7 Ma. (Ribeiro, Stern, Kelley, et al., 2013) with widespread active margin volcanism apparently now waning or ceased, although there are indications of locally continuing activity (Brounce et al., 2016; Stern et al., 2014) suggesting that this age range may be a minimum. Thus, the duration of the main phase of southern Mariana forearc magmatism appears to be short, like that inferred for IBM subduction zone infancy lasting ~2–4 Myr (Ishizuka et al., 2006). We explain the short duration of this phase of volcanism as due to the widening zone of pure shear extension wherein mantle upwelling rates decrease as the basin widens (Buck et al., 1988). Slowing mantle advection together with cooling to the surface and from the underlying slab quickly suppresses mantle melting, despite hydration from the slab. This self-limiting mechanism may explain the short period of widespread and robust volcanism inferred at subduction zone infancy.

Unlike mature forearcs underlain by old slab that are generally cold, limiting shallow thermal breakdown of hydrous slab minerals (Abers et al., 2017), active rifting of the southern Mariana forearc draws hot mantle wedge asthenosphere to very near the trench and slab. Young volcanism close to the trench axis (Ribeiro, Stern, Kelley, et al., 2013) indicates above-solidus thermal conditions in the underlying mantle proximal to the slab. Hot mantle wedge asthenosphere adjacent to the subducting Pacific slab should induce vigorous breakdown of hydrous mineral phases in the slab as indicated by the abundance of fluid mobile slab-derived elements in SEMFR volcanics (Ribeiro, Stern, Martinez, et al., 2013; Ribeiro et al., 2015). Partitioning calculations between strongly hydrous melt and residual mantle in arc settings indicate that even the residual forearc mantle after melt extraction should retain high H^+, unlike at MOR settings where the residual mantle is dehydrated by melting and melt extraction (Hirth & Kohlstedt, 2003). If we further consider that the slab will continue to add more water to the mantle wedge and lithosphere even after mantle wedge temperatures decrease below the solidus and water extraction mechanisms through melting cease, a very hydrous and weak lithosphere is predicted. Extension of weak mantle lithosphere results in broad deformation (Gueydan et al., 2008) that cannot form a focused spreading center, therefore distributing volcanic products in a wide zone. In the southern Mariana margin, broadly distributed tectonic deformation continues, as shown by the distribution of earthquakes (Figure 4).

4.4. Implications for Narrow Plate Boundary Zones and Plate Tectonics

The diffuse deformation of the southern Mariana platelet is unusual for oceanic-type lithosphere. In most oceanic extensional settings, a period of tectonic rifting is followed by a focusing of extension leading to magmatic crustal accretion within a narrow plate boundary zone (seafloor spreading). Typical examples include propagating rifts (Hey et al., 1980) even at large offsets (Hey et al., 1995). When oceanic rifts propagate into older lithosphere, the tectonic rifting phase may be more extensive than in young lithosphere, but once magmatic accretion occurs it tends to rapidly focus to a narrow axis (Martinez et al., 1991; Naar et al., 1991). This is also generally true in shear-dominated convergent margin settings. Typical examples occur at STEP faults (Govers & Wortel, 2005) where subduction zones end against shear margins. Well-studied examples occur in the Northeast Lau Spreading Center (Wright et al., 2000), the East Scotia

Ridge (Livermore, 2003), and the southern New Hebrides trench (Patriat et al., 2015). In each of these settings, a focused spreading center intersects the trench (or nearly so in the New Hebrides case). These spreading centers lie behind the arc volcanic front, however, where the slab is deep and mostly dehydrated between the trench and the arc front volcanoes. The morphologic trench in these settings is primarily a shear zone with limited underlying slab. However, these examples demonstrate that trench-parallel extension of the upper plate abutting a morphologic trench does not in itself lead to diffuse deformation. In the southern Mariana margin a critical difference is that the trench has a significant southward directed rollback component of motion (as indicated by thrust earthquake *p*-axis azimuths; Figure 4) and is completely underlain by actively subducting Pacific plate (Figure S3) that has not previously dewatered elsewhere.

We hypothesize that the broadly distributed nature of southern Mariana margin volcano-tectonic extension reflects the weakening effects of water on mantle rheology (Mei & Kohlstedt, 2000a, 2000b). A few parts per million H^+ ions decrease the viscosity (strength) of olivine aggregates by 2 orders of magnitude or more (Hirth & Kohlstedt, 1996, 2003; Karato et al., 1986). Trench-parallel rifting of the southern Mariana margin directly over an actively subducting slab should produce especially hydrous mantle. At mid-ocean ridges (MORs) mantle water content is low compared to convergent margins (Kelley et al., 2006). On melting, water behaves as an incompatible element and melting and melt extraction at MORs is thought to effectively dehydrate the residual mantle lithosphere leading to a several order of magnitude increase in viscosity of the residual mantle, forming a "compositional" lithosphere (Hirth & Kohlstedt, 1996; Phipps Morgan, 1997). Pressure gradients generated within the deforming and strengthening residual mantle matrix as it undergoes corner flow are thought to help focus melt delivery to the narrow ridge axis (Phipps Morgan, 1997). Beneath the southern Mariana margin, the extending lithosphere is underlain by a dewatering slab. Thus, although melting and melt extraction remove water from the residual mantle (as shown by high water content in erupted lavas (Ribeiro et al., 2015)), slab dewatering provides a continual flux of new water, opposing mantle dehydration from melt extraction (Figure 9b). As the southern Mariana rift widens, mantle advection rates decrease and cooling eventually decreases mantle melting (Figure 9c). However, mantle wedge material near the slab will remain hot enough for a time to induce significant breakdown of hydrous minerals in the slab. Therefore, even after significant melting and volcanism cease, the forearc mantle will continue to be fluxed by slab-derived water, further increasing its water content. Active infiltration of water from the slab into the forearc appears to continue even as forearc mantle cools to lithosphere as shown by active serpentine mud volcanoes (Fryer, 2012) and seeps of slab-derived water (Mottl et al., 2004) in the central Mariana forearc. Residual mantle lithosphere in the southern Mariana margin thus remains weak, as its water content should be much greater even than that of MOR mantle before melting, due to its continual fluxing from the underlying slab (Figure 9).

The diffuse deformation in the southern Mariana margin does not appear to be dependent on the kinematics of the margin, which involve tangential and radial extensional components. An abrupt transition also occurs along the MGR spreading center as it moves over the ~100 km depth contour of the slab, where a greater degree of slab dewatering is predicted in some models (Schmidt & Poli, 1998). Detailed near-bottom side scan sonar mapping shows that the narrow axis of the MGR abruptly transitions to a much broader zone of crustal accretion tens of kilometers wide in the DSZ. Basement fabric in this area indicates primarily trench-perpendicular extension. Similar transitions have been noted at the southern end of the Valu Fa Ridge in the Lau Basin (Martinez & Taylor, 2006), and we have hypothesized that much of the Havre Trough may be undergoing diffuse extension due to ultraslow opening and hydration from the underlying slab (Martinez et al., 2013; Martinez & Sleeper, 2012). Thus, even where extension is primarily parallel to the rollback direction, diffuse deformation occurs. The control on diffuse lithospheric deformation appears to be compositional, based on mantle water content, rather than due to complex or changing kinematics.

The observations from the southern Mariana margin present a test of the dehydration compositional lithosphere model and its predicted effects on the plate boundary zone (Hirth & Kohlstedt, 1996; Phipps Morgan, 1997). Our observations support the conclusion that mantle dehydration beneath mid-ocean ridges is at least a supportive if not necessary process for forming narrow divergent plate boundary zones. At convergent margins underlain by dewatering slabs upper plate mantle dehydration is suppressed if not prevented, hydrous lithosphere remains weak, and the narrow plate boundary zones that characterize plate tectonics cannot form, except farther from the trench within dryer backarc basin lithosphere. Our results also imply that the hydrated lithosphere of convergent margin leading edges is important for understanding their

origin through broadly distributed and contemporaneous volcano-tectonic deformation (Taylor, 1992), including the propensity of convergent margin leading edges to change shape during their evolution so that conjugate margins of backarc basins do not generally fit back together. These observations raise another important question as well: If ophiolites generally originate as forearc terrains through processes of diffuse volcano-tectonic extension as inferred from extensive studies (Bloomer & Hawkins, 1983; Ishizuka et al., 2006; Stern & Bloomer, 1992; Taylor, 1992), how appropriate are ophiolites as analogs for the highly focused plate boundary zones of mid-ocean ridges?

5. Conclusions

Detailed geophysical mapping of the southern Mariana margin together with regional data demonstrates pervasive and broadly distributed volcano-tectonic deformation of the leading margin flank following rifting of the predecessor Eocene-Miocene forearc. This contrasts with the trailing edge on the Philippine Sea plate that behaves rigidly and appears to have been largely accreted through organized seafloor spreading. We hypothesize that the diffuse deformation and crustal accretion of the leading edge of the margin is enabled by hydration from slab-derived fluids that maintain a weak upper plate lithosphere. The southern Mariana margin may thus represent an active analog of the diffuse volcano-tectonic processes inferred at subduction zone infancy to have formed the ~300 km wide zone of contemporaneous Eocene volcanism that characterizes the entire length of the IBM system. The observations have important implications for what enables the narrow plate boundary zones that characterize plate tectonics in general, supporting suggestions that mantle dehydration and strengthening is at least an assisting process. At convergent margins where oceanic lithosphere is infused by hydrous flux from the subducted slab, it remains weak and narrow plate boundary zones cannot form.

Acknowledgments

This collaborative research was funded by NSF grants OCE-0961811 to F. Martinez, OCE-0961559 to K. Kelley, and OCE-0961352 to R.J. Stern. Geophysical data from R/V *Thompson cruise TN273* are available online at http://www.rvdata.us/catalog/TN273. We thank the R/V *Thompson* Captain and crew for their proficient ship operation and T. Ishii and the shipboard science party for their enthusiastic assistance during the cruise. We also thank Brian Taylor for discussions that improved our kinematic model and two anonymous reviewers and Chief Editor Uri ten Brink for their constructive and helpful comments that improved the manuscript. These are HIGP contribution 2279 and SOEST contribution 10316 and UTD Geosciences contribution 1319.

References

Abers, G. A., van Keken, P. E., & Hacker, B. R. (2017). The cold and relatively dry nature of mantle forearcs in subduction zones. *Nature Geoscience*, *10*(5), 333–337. https://doi.org/10.1038/ngeo2922

Arculus, R. J., Ishizuka, O., Bogus, K. A., Gurnis, M., Hickey-Vargas, R., Aljahdali, M. H., … Zhang, Z. (2015). A record of spontaneous subduction initiation in the Izu-Bonin-Mariana arc. *Nature Geoscience*, *8*(9), 728–733. https://doi.org/10.1038/ngeo2515

Armstrong, A. A. (2011). Cruise report USNS sumner, U.S. extended continental shelf cruise to map sections of the Mariana trench and the eastern and southern insular margins of Guam and the Northern Mariana Islands. Retrieved from http://ccom.unh.edu/publications/Armstrong_2011_cruise_report_SU10-02_Marianas.pdf

Auzende, J.-M., Gràcia-Mont, E., Bendel, V., Huchon, P., Lafoy, Y., Lagabrielle, Y., … Tanahashi, M. (1994). A possible triple junction at 14°50′S on the North Fiji Basin Ridge (Southwest Pacific)? *Marine Geology*, *116*(1-2), 25–35. https://doi.org/10.1016/0025-3227(94)90166-X

Becker, N. C., Fryer, P., & Moore, G. F. (2010). Malaguana-Gadao Ridge: Identification and implications of a magma chamber reflector in the southern Mariana Trough. *Geochemistry, Geophysics, Geosystems*, *11*, Q04X13. https://doi.org/10.1029/2009GC002719

Bevis, M. (1986). The curvature of Wadati-Benioff zones and the torsional rigidity of subducting plates. *Nature*, *323*(6083), 52–53. https://doi.org/10.1038/323052a0

Bevis, M. (1988). Seismic slip and down-dip strain rates in Wadati-Benioff zones. *Science*, *240*(4857), 1317–1319. https://doi.org/10.1126/science.240.4857.1317

Billen, M. I., & Gurnis, M. (2001). A low viscosity wedge in subduction zones. *Earth and Planetary Science Letters*, *193*(1-2), 227–236. https://doi.org/10.1016/S0012-821X(01)00482-4

Bird, P. (2003). An updated digital model of plate boundaries. *Geochemistry, Geophysics, Geosystems*, *4*(3), 1027. https://doi.org/10.1029/2001GC000252

Blakely, R. J. (1995). *Potential theory in gravity and magnetic applications*. New York: Cambridge University Press. https://doi.org/10.1017/CBO9780511549816

Bloomer, S. H., & Hawkins, J. W. (1983). Gabbroic and ultramafic rocks from the Mariana trench: An island arc ophiolite. In D. E. Hayes (Ed.), *The tectonic and geologic evolution of the Southeast Asian Seas and Islands: Part 2* (pp. 294–317). Washington, DC: American Geophysical Union. https://doi.org/10.1029/GM027p0294

Bloomer, S. H., Taylor, B., Macleod, C. J., Stern, R. J., Fryer, P., Hawkins, J. W., & Johnson, L. (1995). Early arc volcanism and the ophiolite problem: A perspective from drilling the western Pacific. In B. Taylor & J. Natland (Eds.), *Active margins and marginal basins of the western Pacific* (pp. 1–30). Washington, DC: American Geophysical Union. https://doi.org/10.1029/GM088p0001

Brounce, M. N., Kelley, K. A., & Cottrell, E. (2014). Variations in $Fe^{3+}/\sum Fe$ of Mariana arc basalts and mantle wedge fO_2. *Journal of Petrology*, *55*(12), 2513–2536. https://doi.org/10.1093/petrology/egu065

Brounce, M. N., Kelley, K. A., Stern, R., Martinez, F., & Cottrell, E. (2016). The Fina Nagu Volcanic Complex: Unusual submarine arc volcanism in the rapidly deforming southern Mariana margin. *Geochemistry, Geophysics, Geosystems*, *17*, 4078–4091. https://doi.org/10.1002/2016GC006457

Buck, W. R., Martinez, F., Steckler, M. S., & Cochran, J. R. (1988). Thermal consequences of lithospheric extension: Pure and simple. *Tectonics*, *7*(2), 213–234. https://doi.org/10.1029/TC007i002p00213

Calvert, A. J., Klemperer, S. L., Takahashi, N., & Kerr, B. C. (2008). Three-dimensional crustal structure of the Mariana island arc from seismic tomography. *Journal of Geophysical Research*, *113*, B01406. https://doi.org/10.1029/2007JB004939

Carlson, R. L., & Melia, P. J. (1984). Subduction hinge migration. *Tectonophysics*, *102*(1-4), 399–411. https://doi.org/10.1016/0040-1951(84)90024-6

Carlson, R. L., & Mortera-Gutiérrez, C. A. (1990). Subduction hinge migration along the Izu-Bonin-Mariana Arc. *Tectonophysics*, *181*(1-4), 331–344. https://doi.org/10.1016/0040-1951(90)90026-5

Deschamps, A., & Lallemand, S. (2002). The West Philippine Basin: An Eocene to early Oligocene back arc basin opened between two opposed subduction zones. *Journal of Geophysical Research*, *107*(B12), 2322. https://doi.org/10.1029/2001JB001706

Dewey, J. F. (1980). Episodicity, sequence, and style at convergent plate boundaries. In D. W. Strangway (Ed.), *The continental crust and its mineral deposits* (pp. 554–573). Waterloo, Ontario: Geological Association of Canada.

Dunn, R. A., & Martinez, F. (2011). Contrasting crustal production and rapid mantle transitions beneath back-arc ridges. *Nature*, *469*(7329), 198–202. https://doi.org/10.1038/nature09690

Dziewonski, A. M., Chou, T.-A., & Woodhouse, J. H. (1981). Determination of earthquake source parameters from waveform data for studies of global and regional seismicity. *Journal of Geophysical Research*, *86*(B4), 2825–2852. https://doi.org/10.1029/JB086iB04p02825

Eason, D. E., & Dunn, R. A. (2015). Petrogenesis and structure of oceanic crust in the Lau back-arc basin. *Earth and Planetary Science Letters*, *429*, 128–138. https://doi.org/10.1016/j.epsl.2015.07.065

Edwards, M., Rognstad, M., Tottori, S. N., Davis, R. B., Appelgate, T. B., Johnson, P. D., & Kevis-Sterling, A. (2006). Early results from the IMI-30 towed sonar system, Eos Trans. AGU, (52) Fall Meet. Suppl., Abstract OS33A-1675.

Eguchi, T. (1984). Seismotectonics around the Mariana Trough. *Tectonophysics*, *102*(1-4), 33–52. https://doi.org/10.1016/0040-1951(84)90007-6

Ekström, G., Nettles, M., & Dziewonski, A. M. (2012). The global CMT project 2004-2010: Centroid-moment tensors for 13,017 earthquakes. *Physics of the Earth and Planetary Interiors*, *200-201*, 1–9. https://doi.org/10.1016/j.pepi.2012.04.002

Fryer, P. (2012). Serpentinite mud volcanism: Observations, processes, and implications. In C. A. Carlson & S. J. Giovannoni (Eds.), *Annual review of marine science* (Vol. 4, pp. 345–373). Palo Alto: Annual Reviews.

Fryer, P., Becker, N., Appelgate, B., Martinez, F., Edwards, M., & Fryer, G. (2003). Why is the challenger deep so deep? *Earth and Planetary Science Letters*, *211*(3-4), 259–269. https://doi.org/10.1016/S0012-821X(03)00202-4

Gaetani, G. A., & Grove, T. L. (1998). The influence of water on melting of mantle peridotite. *Contributions to Mineralogy and Petrology*, *131*(4), 323–346. https://doi.org/10.1007/s004100050396

Gamo, T., Masuda, H., Yamanaka, T., Okamura, K., Ishibashi, J., Nakayama, E., … Sano, Y. (2004). Discovery of a new hydrothermal venting site in the southernmost Mariana Arc: Al-rich hydrothermal plumes and white smoker activity associated with biogenic methane. *Geochemical Journal*, *38*(6), 527–534. https://doi.org/10.2343/geochemj.38.527

Goff, J. A. (1991). A global and regional stochastic analysis of near-ridge abyssal hill morphology. *Journal of Geophysical Research*, *96*(B13), 21713–21737. https://doi.org/10.1029/91JB02275

Govers, R., & Wortel, M. J. R. (2005). Lithosphere tearing at STEP faults: Response to edges of subduction zones. *Earth and Planetary Science Letters*, *236*(1-2), 505–523. https://doi.org/10.1016/j.epsl.2005.03.022

Grove, T. L., Till, C. B., & Krawczynski, M. J. (2012). The role of H_2O in subduction zone magmatism. *Annual Review of Earth and Planetary Sciences*, *40*(1), 413–439. https://doi.org/10.1146/annurev-earth-042711-105310

Gueydan, F., Morency, C., & Brun, J.-P. (2008). Continental rifting as a function of lithosphere mantle strength. *Tectonophysics*, *460*(1-4), 83–93. https://doi.org/10.1016/j.tecto.2008.08.012

Hagen, R. A., Shor, A. N., & Fryer, P. (1992). Seamarc ii evidence for the locus of sea-floor spreading in the southern Mariana trough. *Marine Geology*, *103*(1-3), 311–322. https://doi.org/10.1016/0025-3227(92)90022-A

Harrison, C. G. A. (1987). Marine magnetic anomalies—The origin of the stripes. *Annual Review of Earth and Planetary Sciences*, *15*(1), 505–543. https://doi.org/10.1146/annurev.ea.15.050187.002445

Hayes, G. P., Wald, D. J., & Johnson, R. L. (2012). Slab1.0: A three-dimensional model of global subduction zone geometries. *Journal of Geophysical Research*, *117*, B01302. https://doi.org/10.1029/2011JB008524

Hey, R. N., Duennebier, F. K., & Morgan, W. J. (1980). Propagating rifts on mid-ocean ridges. *Journal of Geophysical Research*, *85*(B7), 3647–3658. https://doi.org/10.1029/JB085iB07p03647

Hey, R. N., Johnson, P. D., Martinez, F., Korenaga, J., Somers, M. L., Huggett, Q. J., … Naar, D. F. (1995). Plate boundary reorganization at a large-offset, rapidly propagating rift. *Nature*, *378*(6553), 167–170. https://doi.org/10.1038/378167a0

Hirth, G., & Kohlstedt, D. L. (1996). Water in the oceanic upper mantle: Implications for rheology, melt extraction and the evolution of the lithosphere. *Earth and Planetary Science Letters*, *144*(1-2), 93–108. https://doi.org/10.1016/0012-821X(96)00154-9

Hirth, G., & Kohlstedt, D. (2003). Rheology of the upper mantle and the mantle wedge: A view from the experimentalists. In J. Eiler (Ed.), *Inside the subduction factory* (pp. 83–105). Washington DC: American Geophysical Union. https://doi.org/10.1029/138GM06

Hussong, D. M., & Uyeda, S. (1981). Tectonic processes and the history of the Mariana arc: A synthesis of the results of Deep Sea Drilling Project Leg 60. In D. M. Hussong & S. Uyeda (Eds.), *Initial Reports of the Deep Sea Drilling Project* (pp. 909–929). Washington DC: U. S. Government Printing Office.

Hyndman, R. D., & Peacock, S. M. (2003). Serpentinization of the forearc mantle. *Earth and Planetary Science Letters*, *212*(3-4), 417–432. https://doi.org/10.1016/S0012-821X(03)00263-2

International Seismological Centre (2014). International Seismological Centre On-line Bulletin, Thatcham, United Kingdom. Retrieved from http://www.isc.ac.uk

Ishizuka, O., Kimura, J.-I., Li, Y. B., Stern, R. J., Reagan, M. K., Taylor, R. N., … Haraguchi, S. (2006). Early stages in the evolution of Izu-Bonin arc volcanism: New age, chemical, and isotopic constraints. *Earth and Planetary Science Letters*, *250*(1-2), 385–401. https://doi.org/10.1016/j.epsl.2006.08.007

Karato, S.-I., Patterson, M. S., & Fitz Gerald, J. D. (1986). Rheology of synthetic olivene aggregates: Influence of grain size and water. *Journal of Geophysical Research*, *91*(B8), 8151–8176. https://doi.org/10.1029/JB091iB08p08151

Karig, D. E. (1972). Remnant arcs. *Bulletin of the Geological Society of America*, *83*(4), 1057–1068. https://doi.org/10.1130/0016-7606(1972)83%5B1057:RA%5D2.0.CO;2

Karig, D. E., Anderson, R. N., & Bibee, L. D. (1978). Characteristics of back arc spreading in the Mariana trough. *Journal of Geophysical Research*, *83*(B3), 1213–1226. https://doi.org/10.1029/JB083iB03p01213

Kato, T., Beavan, J., Matsushima, T., Kotake, Y., Camacho, J. T., & Nakao, S. (2003). Geodetic evidence of back-arc spreading in the Mariana Trough. *Geophysical Research Letters*, *30*(12), 1625. https://doi.org/10.1029/2002GL016757

Kelley, K. A., Plank, T., Grove, T. L., Stolper, E. M., Newman, S., & Hauri, E. (2006). Mantle melting as a function of water content beneath back-arc basins. *Journal of Geophysical Research*, *111*, B09208. https://doi.org/10.1029/2005JB003732

Kelley, K. A., Plank, T., Newman, S., Stolper, E. M., Grove, T. L., Parman, S., & Hauri, E. H. (2010). Mantle melting as a function of water content beneath the Mariana Arc. *Journal of Petrology*, *51*(8), 1711–1738. https://doi.org/10.1093/petrology/egq036

Kitada, K., Seama, N., Yamazaki, T., Nogi, Y., & Suyehiro, K. (2006). Distinct regional differences in crustal thickness along the axis of the Mariana Trough, inferred from gravity anomalies. *Geochemistry, Geophysics, Geosystems*, *7*, Q04011. https://doi.org/10.1029/2005GC001119

Kobayashi, K. (2004). Origin of the Palau and Yap trench-arc systems. *Geophysical Journal International*, *157*(3), 1303–1315. https://doi.org/10.1111/j.1365-246X.2003.02244.x

Kuo, B.-Y., & Forsyth, D. W. (1988). Gravity anomalies of the ridge-transform system in the south Atlantic between 31 and 34.5°S: Upwelling centers and variations in crustal thickness. *Marine Geophysical Researches*, *10*(3-4), 205–232. https://doi.org/10.1007/BF00310065

Lafoy, Y., Auzende, J. M., Ruellan, E., Huchon, P., & Honza, E. (1990). The 16°40′ S triple junction in the North Fiji Basin (SW Pacific). *Marine Geophysical Researches*, *12*(4), 285–296. https://doi.org/10.1007/BF02428199

Lesur, V., Hamoudi, M., Choi, Y., Dyment, J., & Thébault, E. (2016). Building the second version of the World Digital Magnetic Anomaly Map (WDMAM). *Earth, Planets and Space*, *68*(1), 27. https://doi.org/10.1186/s40623-016-0404-6

Livermore, R. (2003). Back-arc spreading and mantle flow in the East Scotia Sea. In R. Larter & P. Leat (Eds.), *Intra-oceanic subduction systems: Tectonic and magmatic processes* (pp. 315–331). London: Geological Society, Special Publications 219.

Luis, J. F. (2007). Mirone: A multi-purpose tool for exploring grid data. *Computers & Geosciences*, *33*(1), 31–41. https://doi.org/10.1016/j.cageo.2006.05.005

Martinez, F., & Sleeper, J. D. (2012). Influence of arc proximity on back-arc seafloor spreading, 34th International Geological Congress 2012, Brisbane, Australia.

Martinez, F., & Taylor, B. (2002). Mantle wedge control on back-arc crustal accretion. *Nature*, *416*(6879), 417–420. https://doi.org/10.1038/416417a

Martinez, F., & Taylor, B. (2003). Controls on back-arc crustal accretion: Insights from the Lau, Manus and Mariana basins. In R. D. Larter & P. T. Leat (Eds.), *Intra-oceanic subduction systems: Tectonic and magmatic processes* (pp. 19–54). London: Geological Society of London.

Martinez, F., & Taylor, B. (2006). Modes of crustal accretion in back-arc basins: Inferences from the Lau Basin. In D. M. Christie, C. R. Fisher, S.-M. Lee, & S. Givens (Eds.), *Back-arc spreading systems: Geological, biological, chemical and physical Interactions*, *Geophyscial Monograph Series* (Vol. 166, pp. 5–30). Washington, DC: American Geophysical Union. https://doi.org/10.1029/166GM03

Martinez, F., Naar, D. F., Reed, T. B., & Hey, R. N. (1991). Three-dimensional SeaMARC II, gravity, and magnetics study of large-offset rift propagation at the Pito Rift, Easter Microplate. *Marine Geophysical Researches*, *13*(4), 255–285. https://doi.org/10.1007/BF00366279

Martinez, F., Fryer, P., & Becker, N. (2000). Geophysical characteristics of the southern Mariana trough, 11°50′N–13°40′N. *Journal of Geophysical Research*, *105*(B7), 16,591–16,607. https://doi.org/10.1029/2000JB900117

Martinez, F., Taylor, B., Baker, E. T., Resing, J. A., & Walker, S. L. (2006). Opposing trends in crustal thickness and spreading rate along the back-arc Eastern Lau Spreading Center: Implications for controls on ridge morphology, faulting, and hydrothermal activity. *Earth and Planetary Science Letters*, *245*(3-4), 655–672. https://doi.org/10.1016/j.epsl.2006.03.049

Martinez, F., Dunn, R. A., & Sleeper, J. D. (2013). Seafloor spreading in the Lau-Havre Backarc Basins: From fast to ultra slow, American Geophysical Union Fall Meeting 2013, Abstract V21C-2739, San Francisco, CA.

Masuda, H., & Fryer, P. (2015). Geochemical characteristics of active backarc basin volcanism at the southern end of the Mariana Trough. In J.-i. Ishibashi, K. Okino, & M. Sunamura (Eds.), *Subseafloor biosphere linked to hydrothermal systems: TAIGA Concept* (pp. 261–273). Tokyo: Springer Japan.

Maus, S., & Macmillan, S. (2005). Geomagnetism and paleomagnetism: 10th Generation International Geomagnetic Reference Field. *Eos, Transactions American Geophysical Union*, *86*(16), 159. https://doi.org/10.1029/2005EO160006

Mei, S., & Kohlstedt, D. L. (2000a). Influence of water on plastic deformation of olivine aggregates: 1. Diffusion creep regime. *Journal of Geophysical Research*, *105*(B9), 21,457–21,469. https://doi.org/10.1029/2000JB900179

Mei, S., & Kohlstedt, D. L. (2000b). Influence of water on plastic deformation of olivine aggregates: 2. Dislocation creep regime. *Journal of Geophysical Research*, *105*(B9), 21,471–21,481. https://doi.org/10.1029/2000JB900180

Molnar, P., & Atwater, T. (1978). Interarc spreading and Cordilleran tectonics as alternates related to the age of subducted oceanic lithosphere. *Earth and Planetary Science Letters*, *41*(3), 330–340. https://doi.org/10.1016/0012-821X(78)90187-5

Mottl, M. J., Wheat, C. G., Fryer, P., Gharib, J., & Martin, J. B. (2004). Chemistry of springs across the Mariana forearc shows progressive devolatilization of the subducting plate. *Geochimica et Cosmochimica Acta*, *68*(23), 4915–4933. https://doi.org/10.1016/j.gca.2004.05.037

Naar, D. F., Martinez, F., Hey, R., Reed, T. B., & Stein, S. (1991). Pito rift: How a large-offset rift propagates. *Marine Geophysical Research*, *13*(4), 287–309. https://doi.org/10.1007/BF00366280

Ohara, Y., & Ishii, T. (1998). Peridotites from the southern Mariana forearc: Heterogeneous fluid supply in mantle wedge. *Island Arc*, *7*(3), 541–558. https://doi.org/10.1111/j.1440-1738.1998.00209.x

Ohara, Y., Reagan, M. K., Fujikura, K., Watanabe, H., Michibayashi, K., Ishii, T., … Kino, M. (2012). A serpentinite-hosted ecosystem in the Southern Mariana Forearc. *Proceedings of the National Academy of Sciences of the United States of America*, *109*(8), 2831–2835. https://doi.org/10.1073/pnas.1112005109

Okino, K., Shimakawa, Y., & Nagaoka, S. (1994). Evolution of the Shikoku Basin. *Journal of Geomagnetism and Geoelectricity*, *46*(6), 463–479. https://doi.org/10.5636/jgg.46.463

Okino, K., Kasuga, S., & Ohara, Y. (1998). A new scenario of the Parece Vela Basin genesis. *Marine Geophysical Researches*, *20*(1), 21–40. https://doi.org/10.1023/A:1004377422118

Parker, R. L. (1972). The rapid calculation of potential anomalies. *Geophysical Journal of the Royal Astronomical Society*, *31*, 447–455.

Parker, R. L., & Huestis, S. P. (1974). The inversion of magnetic anomalies in the presence of topography. *Journal of Geophysical Research*, *79*(11), 1587–1593. https://doi.org/10.1029/JB079i011p01587

Parsons, B., & Sclater, J. G. (1977). An analysis of the variation of ocean floor bathymetry and heat flow with age. *Journal of Geophysical Research*, *82*(5), 803–827. https://doi.org/10.1029/JB082i005p00803

Patriat, M., Collot, J., Danyushevsky, L., Fabre, M., Meffre, S., Falloon, T., … Fournier, M. (2015). Propagation of back-arc extension into the arc lithosphere in the southern New Hebrides volcanic arc. *Geochemistry, Geophysics, Geosystems*, *16*(9), 3142–3159. https://doi.org/10.1002/2015GC005717

Pelletier, B., Calmant, S., & Pillet, R. (1998). Current tectonics of the Tonga-New Hebrides region. *Earth and Planetary Science Letters*, *164*(1-2), 263–276. https://doi.org/10.1016/S0012-821X(98)00212-X

Perram, L. J., Cormier, M.-H., & Macdonald, K. C. (1993). Magnetic and tectonic studies of the dueling propagating spreading centers at 20°40′S on the East Pacific Rise: Evidence for crustal rotations. *Journal of Geophysical Research*, *98*(B8), 13,835–13,850. https://doi.org/10.1029/92JB02913

Phipps Morgan, J. (1997). The generation of a compositional lithosphere by mid-ocean ridge melting and its effect on subsequent off-axis hotspot upwelling and melting. *Earth and Planetary Science Letters*, *146*(1-2), 213–232. https://doi.org/10.1016/S0012-821X(96)00207-5

Reagan, M. K., Ishizuka, O., Stern, R. J., Kelley, K. A., Ohara, Y., Blichert-Toft, J., … Woods, M. (2010). Fore-arc basalts and subduction initiation in the Izu-Bonin-Mariana system. *Geochemistry, Geophysics, Geosystems*, *11*, Q03X12. https://doi.org/10.1029/2009GC002871

Reagan, M. K., McClelland, W. C., Girard, G., Goff, K. R., Peate, D. W., Ohara, Y., & Stern, R. J. (2013). The geology of the southern Mariana fore-arc crust: Implications for the scale of Eocene volcanism in the western Pacific. *Earth and Planetary Science Letters*, *380*(0), 41–51. https://doi.org/10.1016/j.epsl.2013.08.013

Reagan, M. K., Pearce, J. A., Petronotis, K., Almeev, R. R., Avery, A. J., Carvallo, C., … Whattam, S. A. (2017). Subduction initiation and ophiolite crust: New insights from IODP drilling. *International Geology Review*, *59*(11), 1439–1450.

Ribeiro, J. M., Stern, R. J., Martinez, F., Ishizuka, O., Merle, S. G., Kelley, K., … Bloomer, S. (2013). Geodynamic evolution of a forearc rift in the southernmost Mariana Arc. *Island Arc*, *22*(4), 453–476. https://doi.org/10.1111/iar.12039

Ribeiro, J. M., Stern, R. J., Kelley, K. A., Martinez, F., Ishizuka, O., Manton, W. I., & Ohara, Y. (2013). Nature and distribution of slab-derived fluids and mantle sources beneath the Southeast Mariana forearc rift. *Geochemistry, Geophysics, Geosystems*, *14*, 4585–4607. https://doi.org/10.1002/ggge.20244

Ribeiro, J. M., Stern, R. J., Kelley, K. A., Shaw, A. M., Martinez, F., & Ohara, Y. (2015). Composition of the slab-derived fluids released beneath the Mariana forearc: Evidence for shallow dehydration of the subducting plate. *Earth and Planetary Science Letters*, *418*, 136–148. https://doi.org/10.1016/j.epsl.2015.1002.1018

Ribeiro, J. M., Stern, R. J., Martinez, F., Woodhead, J., Chen, M., & Ohara, Y. (2017). Asthenospheric outflow from the shrinking Philippine Sea Plate: Evidence from Hf–Nd isotopes of southern Mariana lavas. *Earth and Planetary Science Letters*, *478*, 258–271. https://doi.org/10.1016/j.epsl.2017.1008.1022

Rognstad, M., Appelgate, B., & Ericksen, T. (2003). The IMI-30 seafloor imaging system: Development of a new NSF deep-towed 30 kHz bathymetric sidescan sonar system, Eos Trans. AGU, 84 (46) Fall Meet. Suppl.(46), Abstract OS32A-0239.

Sandwell, D. T., Müller, R. D., Smith, W. H. F., Garcia, E., & Francis, R. (2014). New global marine gravity model from CryoSat-2 and Jason-1 reveals buried tectonic structure. *Science*, *346*(6205), 65–67. https://doi.org/10.1126/science.1258213

Schellart, W. P. (2004). Kinematics of subduction and subduction-induced flow in the upper mantle. *Journal of Geophysical Research*, *109*, B07401. https://doi.org/10.1029/2004JB002970

Schellart, W. P., & Moresi, L. (2013). A new driving mechanism for backarc extension and backarc shortening through slab sinking induced toroidal and poloidal mantle flow: Results from dynamic subduction models with an overriding plate. *Journal of Geophysical Research: Solid Earth*, *118*, 3221–3248. https://doi.org/10.1002/jgrb.50173

Schmidt, M. W., & Poli, S. (1998). Experimentally based water budgets for dehydrating slabs and consequences for arc magma generation. *Earth and Planetary Science Letters*, *163*(1-4), 361–379. https://doi.org/10.1016/S0012-821X(98)00142-3

Seama, N., & Okino, K. (2015). Asymmetric seafloor spreading of the southern Mariana trough back-arc basin. In J.-i. Ishibashi, K. Okino, & M. Sunamura (Eds.), *Subseafloor biosphere linked to hydrothermal systems: TAIGA Concept* (pp. 253–260). Tokyo: Springer Japan.

Seno, T., & Maruyama, S. (1984). Paleogeographic reconstructions and origin of the Philippine Sea. *Tectonophysics*, *102*(1-4), 53–84. https://doi.org/10.1016/0040-1951(84)90008-8

Shin, Y. H., Choi, K. S., & Xu, H. (2006). Three-dimensional forward and inverse models for gravity fields based on the fast Fourier transform. *Computers & Geosciences*, *32*(6), 727–738. https://doi.org/10.1016/j.cageo.2005.10.002

Smith, W. H. F., & Wessel, P. (1990). Gridding with continuous curvature splines in tension. *Geophysics*, *55*(3), 293–305. https://doi.org/10.1190/1.1442837

Stern, R. J., & Bloomer, S. H. (1992). Subduction zone infancy: Examples from the Eocene Izu-Bonin-Mariana and Jurassic California Arcs. *Bulletin of the Geological Society of America*, *104*(12), 1621–1636. https://doi.org/10.1130/0016-7606(1992)104%3C1621:SZIEFT%3E2.3.CO;2

Stern, R. J., & Smoot, N. C. (1998). A bathymetric overview of the Mariana forearc. *The Island Arc*, *7*(3), 525–540. https://doi.org/10.1111/j.1440-1738.1998.00208.x

Stern, R. J., Reagan, M., Ishizuka, O., Ohara, Y., & Whattam, S. (2012). To understand subduction initiation, study forearc crust: To understand forearc crust, study ophiolites. *Lithosphere*, *4*(6), 469–483. https://doi.org/10.1130/L183.1

Stern, R. J., Ren, M., Kelley, K. A., Ohara, Y., Martinez, F., & Bloomer, S. H. (2014). Basaltic volcaniclastics from the Challenger Deep forearc segment, Mariana convergent margin: Implications for tectonics and magmatism of the southernmost Izu–Bonin–Mariana arc. *Island Arc*, *23*(4), 368–382. https://doi.org/10.1111/iar.12088

Stolper, E., & Newman, S. (1994). The role of water in the petrogenesis of Mariana trough magmas. *Earth and Planetary Science Letters*, *121*(3-4), 293–325. https://doi.org/10.1016/0012-821X(94)90074-4

Tatsumi, Y. (1986). Formation of the volcanic front in subduction zones. *Geophysical Research Letters*, *13*(8), 717–720. https://doi.org/10.1029/GL013i008p00717

Taylor, B. (1992). Rifting and the volcanic-tectonic evolution of the Izu-Bonin-Mariana arc. In B. Taylor, et al. (Eds.), *Proceedings of the Ocean Drilling Program, Scientific Results* (Vol. 126, pp. 627–651). College Station, TX: Ocean Drilling Program. https://doi.org/10.2973/odp.proc.sr.126.163.1992

Taylor, B., & Martinez, F. (2003). Back-arc basin basalt systematics. *Earth and Planetary Science Letters*, *210*(3-4), 481–497. https://doi.org/10.1016/S0012-821X(03)00167-5

Wallace, L. M., Ellis, S., & Mann, P. (2009). Collisional model for rapid fore-arc block rotations, arc curvature, and episodic back-arc rifting in subduction settings. *Geochemistry, Geophysics, Geosystems*, *10*, Q05009. https://doi.org/10.1029/2008GC002220

Watts, A. B., & Talwani, M. (1975). Gravity effect of downgoing lithospheric slabs beneath island arcs. *Bulletin of the Geological Society of America*, *86*(1), 1–4. https://doi.org/10.1130/0016-7606(1975)86%3C1:GEODLS%3E2.0.CO;2

Wegner, A. (1966). *The origin of continents and oceans*. New York: Dover Pulications.

Wessel, J. K., Fryer, P., Wessel, P., & Taylor, B. (1994). Extension in the northern Mariana inner forearc. *Journal of Geophysical Research*, *99*(B8), 15,181–15,203. https://doi.org/10.1029/94JB00692

Wessel, P., Smith, W. H. F., Scharroo, R., Luis, J., & Wobbe, F. (2013). Generic Mapping Tools: Improved version released. *Geoskrifter*, *94*(45), 409–410.

Wright, D. J., Bloomer, S. H., MacLeod, C. J., Taylor, B., & Goodliffe, A. M. (2000). Bathymetry of the Tonga trench and forearc: A map series. *Marine Geophysical Researches*, *21*(5), 489–512. https://doi.org/10.1023/A:1026514914220